

The authors thank the editor and referees to review our manuscript and particularly for the valuable comments and suggestions that have significantly improved the manuscript. We provide below point-by-point responses to the referees' comments. We also have made most of the changes suggested by the referees in the revised manuscript.

Referee #1

This manuscript reports the measurements of non-refractory fine particulate matter (NR-PM₁) in Shijiazhuang, China, using a quadrupole aerosol chemical speciation monitor (Q-ACSM). Positive matrix factorization (PMF) analysis is performed for source apportionment of organic aerosol (OA). It is found that on average primary emissions are the major source of NR-PM₁, but secondary pollutants via aqueous phase reactions play a more important role in polluted events. The data analysis is routine and the conclusions are broadly consistent with many previous studies in the same region. Overall, I recommend publication after major revisions.

Major Comments

1. Page 11 Line 4-5. The coal combustion OA (CCOA) is identified based on PAH-related ion peaks in its mass spectrum and the assumption that PAH is mainly from coal combustion. So it is problematic to draw the conclusion that "the major source of PAHs was coal combustion".

Response: PAHs are emitted from coal combustion, biomass burning and vehicular emissions, and PAH-related ions are assigned in these sources in the PMF source apportionment. We did not make the assumption that PAH is mainly from coal combustion, and the assignment is from PMF model runs. For example, in our previous study (Elser et al., 2016a), from PMF study we quantified that the main source of PAHs was biomass burning in Xi'an and was coal combustion in Beijing during severe haze events. In the present study, the PMF model results show that CCOA accounts for 42-66% of PAH-related ions and BBOA accounts for 9-27% of PAH-related ions. We therefore concluded that "this result suggested that the major source of PAHs was coal combustion in wintertime Shijiazhuang."

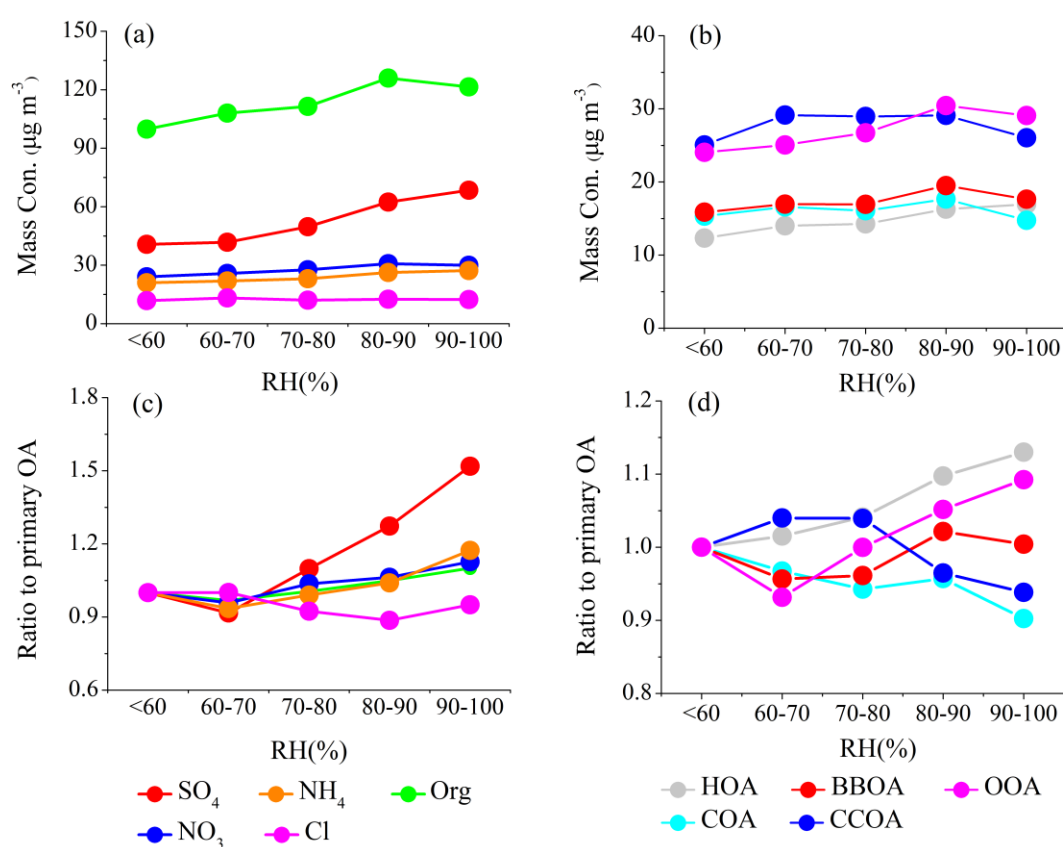
2. Page 11 Line 5-6. As the CCOA concentration is similar between Beijing and Shijiazhuang, does it suggest that the major source of CCOA in Beijing is from local emissions? In the introduction (Page 4 Line 5-15), it is mentioned that previous studies estimate a large fraction of PM in Beijing arising from regional transport. If so, one would imagine that the CCOA concentration is higher in surrounding area, like Hebei, than Beijing.

Response: The average mass concentration of CCOA was similar between Shijiazhuang and Beijing, but they were campaign-averaged concentrations including clean and haze events. In Beijing, the clean periods were generally associated with northerly and northwesterly winds (i.e., from the clean mountain area), while haze extremes were related to southerly winds (i.e., from the polluted southern Hebei including Shijiazhuang). We revisited our data and found that, during haze extremes in the same winter, the average CCOA concentration was 77.5 $\mu\text{g m}^{-3}$ in Shijiazhuang, much higher than that in Beijing (48.2 $\mu\text{g m}^{-3}$).

In the revised manuscript, we have added “Nevertheless, during haze extremes, the average CCOA concentration was $77.5 \mu\text{g m}^{-3}$ in Shijiazhuang, much higher than that in Beijing ($48.2 \mu\text{g m}^{-3}$, Elser et al., 2016a).”

3. Section 3.4. The increase in SO_4/POA and OOA/POA is largely due to the decrease in POA at high RH (90-100% bin). What causes the decrease in POA concentration? Precipitation? Have the precipitation events been excluded from the analysis? In Figure 7, the light blue should be COA, instead of CCOA.

Response: We thanks the referee to point out the flaws. Indeed, the decrease in POA at the RH 90-100% bin was caused by snow. We have excluded the data from snow events in the revised manuscript, and Figure 7 has been updated accordingly (see below). Also, we have changed the light blue from CCOA to COA.



4. Could the authors provide more explanations regarding why POA is important in low RH polluted days, but SOA is important in high RH polluted days? I would imagine that the POA emissions do not vary with RH. Then where does the POA go in high RH polluted days?

Response: This conclusion was drawn based on the mass fraction contribution. During high RH pollution events, more SOA and SIA were formed and therefore their fractional contribution increased. The POA concentrations are determined by both emissions and meteorological conditions.

In the revised manuscript, we have added “...at high RH pollution events likely due to

enhanced secondary formation,”; and “The concentrations of POA are determined by both emissions and meteorological conditions. The different significance of primary aerosol and secondary aerosol in low and high RH pollution events highlights the importance of meteorological conditions in driving particulate pollution.”

According to Figures 1 and 8, there is larger variation in the OA concentration between the six high RH events than the variation between four low RH events. H3, H5, and L3 seem to be outliers.

Response: The OA concentrations are determined by emissions, secondary formation, and meteorological conditions. The larger variation in the OA concentrations/sources between the six high RH events is most likely due to SOA formation. The relatively smaller variation in the OA concentrations/sources between the four low RH events is likely related to stagnant air which facilitates the accumulation of particles.

For H3, H5, and L3 events, each spanned relatively long period (from ~12 hr to ~108 hr). They are real measurement data, not outliers.

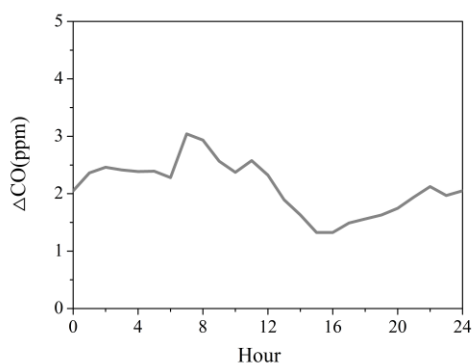
Minor Comments

1. Page 2 Line 21. “Concentration” should be plural.

Response: Change made.

2. Page 8 Line 21. What’s the diurnal trend of delta_CO? Are there rush hour peaks?

Response: The diurnal trend of delta_CO is shown below. There are rush hour peaks.



3. Page 9 Line 5-24. From my understanding, these paragraphs discuss results from unconstrained PMF, right? If so, please be more specific.

Response: From Line 5-11, we discussed the standard PMF results (without constraints); from Line 11-24, we explained which factors were constrained.

4. Page 12 Line 27. Change “compounded” to “confounded”.

Response: Change made.

Referee #2

The authors present a valuable dataset from aerosol mass spectrometry measurements in Shijiazhuang, Hebei, China during the winter of 2014. They have applied the ME-2

approach for more accurate identification of sources. In my assessment the article will be suitable for publication in ACP after a few minor points are addressed:

- This article is closely related to Zhu et al. AMT 2018, which also presents ME-2 analysis of organic aerosol mass spectrometry data from China. The two articles share some of the same authors, and Zhu et al. was available online in final form prior to this article appearing in APCD. That article should be cited and discussed as appropriate in this manuscript.

Response: In the revised manuscript, the article from Zhu et al., 2018 has been cited properly.

- Low FSO₄ does not necessarily indicate low oxidative power in the atmosphere. SO₂ oxidation may occur through a number of multiphase pathways, and other parameters such as aerosol or cloud water pH are more likely to influence FSO₄. Please amend the statements regarding the implications of low FSO₄ throughout the manuscript in light of this caveat.

Response: We agree with the reviewer that sulfate formation may occur through different pathways, including gas-phase oxidation of SO₂ by OH and multiphase reactions of SO₂ with dissolved ozone, hydrogen peroxide, organic peroxides, NO₂, and OH via catalytic or non-catalytic pathways involving mineral oxides. However, these reactions are oxidation reactions, and here we used FSO₄ to represent the oxidation ratio of sulfate. The low oxidation ratio of FSO₄ suggests low atmospheric oxidative capacity. We think such statement is appropriate. Certainly, the absolute mass concentration of sulfate may also be affected by other parameters including aerosol liquid water content, aerosol or cloud water pH.

In the revised manuscript, we have added “Certainly, it should be noted that the mass concentration of sulfate may also be affected by other parameters including aerosol liquid water content, aerosol or cloud water pH, besides atmospheric oxidative capacity.”

- The 1.36e6 premature deaths figure is out of date at this point - please refer to a more recent study such as Cohen et al. Lancet 2017 or Burnett et al. PNAS 2018.

Response: We have made change “1.1 million deaths in 2015 in China”, following the results in Cohen et al., 2017.

- Can anything be inferred from these results regarding the impacts of regional pollution on PM in Beijing?

Response: This study was mainly concentrated on the chemical characteristics, primary emissions and secondary formation processes of aerosol in Shijiazhuang, which is located in the west to Beijing. It certainly will be of interest to investigate the impacts of regional pollution on PM in Beijing, and such studies would need synchronous measurements in Beijing and Shijiazhuang.

- page 5 line 8: 15 March of the next year

Response: Change made.

- page 5 line 9: 2013-2014

Response: Change made.

- page 14 line 10: thermally labile

Response: Change made.

- the Conclusion section is too repetitive, please revise to be more distinct from the Abstract and other sections of the paper

Response: We have shortened the conclusion section.

1 Primary emissions versus secondary formation of fine particulate matter in the top polluted
2 city, Shijiazhuang, in North China

3 Ru-Jin Huang¹, Yichen Wang¹, Junji Cao¹, Chunshui Lin^{1,2}, Jing Duan¹, Qi Chen³, Yongjie Li⁴,
4 Yifang Gu¹, Jin Yan¹, Wei Xu^{1,2}, Roman Fröhlich⁵, Francesco Canonaco⁵, Carlo Bozzetti⁵, Jurgita
5 Ovadnevaite², Darius Ceburnis², Manjula R. Canagaratna⁶, John Jayne⁶, Douglas R. Worsnop⁶, Imad
6 El-Haddad⁵, André S. H. Prévôt⁵, Colin D. O'Dowd²

7 ¹Key Laboratory of Aerosol Chemistry and Physics, Center for Excellence in Quaternary Science and
8 Global Change, and State Key Laboratory of Loess and Quaternary Geology, Institute of Earth
9 Environment, Chinese Academy of Sciences, Xi'an 710061, China

10 ²School of Physics and Centre for Climate and Air Pollution Studies, National University of Ireland
11 Galway, Galway, Ireland

12 ³State Key Joint Laboratory of Environmental Simulation and Pollution Control, College of
13 Environmental Sciences and Engineering, Peking University, Beijing, China

14 ⁴Department of Civil and Environmental Engineering, Faculty of Science and Technology, University
15 of Macau, Taipa, Macau, China

16 ⁵Laboratory of Atmospheric Chemistry, Paul Scherrer Institute (PSI), 5232 Villigen, Switzerland

17 ⁶Aerodyne Research, Inc., Billerica, MA, USA

18 *Correspondence to:* R.-J. Huang (rujin.huang@ieecas.cn)

19 **Abstract.** Particulate matter (PM) pollution is a severe environmental problem in the Beijing-Tianjin-
20 Hebei (BTH) region in North China. PM studies have been conducted extensively in Beijing, but the
21 chemical composition, sources, and atmospheric processes of PM are still relatively less known in the
22 nearby Tianjin and Hebei. In this study, fine PM in urban Shijiazhuang (the capital of Hebei province)
23 was characterized using an Aerodyne quadrupole aerosol chemical speciation monitor (Q-ACSM)
24 from 11 January to 18 February in 2014. The average mass concentration of non-refractory submicron
25 PM (diameter <1 μm , NR-PM₁) was $178 \pm 101 \mu\text{g m}^{-3}$ and composed of 50% organic aerosol (OA),

1 21% sulfate, 12% nitrate, 11% ammonium, and 6% chloride. Using the Multilinear Engine (ME-2)
2 receptor model, five OA sources were identified and quantified, including hydrocarbon-like OA from
3 vehicle emissions (HOA, 13%), cooking OA (COA, 16%), biomass burning OA (BBOA, 17%), coal
4 combustion OA (CCOA, 27%), and oxygenated OA (OOA, 27%). We found that secondary
5 formation contributed substantially to PM in episodic events, while primary emissions were dominant
6 (most significant) on average. The episodic events with the highest NR-PM₁ mass range of 300-360
7 $\mu\text{g m}^{-3}$ showed 55% of secondary species. On the contrary, a campaign-average low OOA fraction
8 (27%) in OA indicated the importance of primary emissions, and a low sulfur oxidation degree (F_{SO_4})
9 of 0.18 even at RH>90% hinted on insufficient oxidation. These results suggested that in wintertime
10 Shijiazhuang fine PM was mostly from primary emissions without sufficient atmospheric aging,
11 indicating opportunities for air quality improvement by mitigating direct emissions. In addition,
12 secondary inorganic and organic (OOA) species dominated in pollution events with high RH
13 conditions, most likely due to enhanced aqueous-phase chemistry, while primary organic aerosol
14 (POA) dominated in pollution events with low RH and stagnant conditions. These results also
15 highlighted the importance of meteorological conditions for PM pollution in this highly polluted city
16 in North China.

17 **1 Introduction**

18 Particulate pollution in China is a serious environmental problem, influencing air quality, regional and
19 global climate and human health. Especially during recent winters, large-scale and severe haze
20 pollution has brought China's particulate pollution at the forefront of world-wide media and evoking
21 great scientific interest in air pollution studies. Measurements at a number of major cities showed that
22 the wintertime daily average mass concentrations of PM_{2.5} (particulate matter with an aerodynamic
23 diameter <2.5 μm) are approximately 1-2 orders of magnitude higher than those observed in urban
24 areas in the US and European countries (Huang et al., 2014). Severe particulate pollution is often
25 accompanied by extremely poor visibility and poor air quality leading to a sharp increase in
26 respiratory diseases. Long-term exposure to high levels of particulate pollution is estimated to result

1 in ~~1.14~~ 1.36 million premature deaths ~~in 2015~~ per year in China, ranking the 1st in the world (Lelieveld
2 et al., 2015; Cohen et al., 2017).

3 The region of Beijing, Tianjin, and Hebei (BTH) is one of the important city clusters in China, but
4 also suffers from serious air pollution. Seven cities in this region ranked the top 10 most polluted
5 cities in China in the year 2014-2015 (<http://www.zhb.gov.cn>). The urgent need of an air quality
6 improvement in this region has been recognized by central and local governments as well as the
7 public, leading to mitigating actions being undertaken by the authorities. In particular, various
8 emission control measures were implemented in this region to clean Beijing's ~~air~~ sky, for example,
9 during the 2014 Asia-Pacific Economic Cooperation (APEC) summit. These temporal measures
10 include the odd-even ban on vehicles and shutdowns of factories and construction sites, leading to
11 serious side effects on daily life and economic growth. Therefore, identification of the major sources
12 and atmospheric processes producing airborne particles is required for implementing targeted and
13 optimized emission control strategies.

14 The first step for quantifying the PM sources requires the measurements of inorganic and organic
15 tracers and/or mass spectrometric fingerprints of ambient PM samples. This can be realized by the
16 online ambient measurements using aerosol mass spectrometric (AMS) techniques to determine
17 aerosol composition (Jimenez et al., 2009; Ng et al., 2011b; Elser et al., 2016b). In particular, the
18 quadrupole aerosol chemical speciation monitor (Q-ACSM) and recently time-of-flight aerosol
19 chemical speciation monitor (TOF-ACSM) have been developed for long-term continuous
20 measurements of the non-refractory submicron aerosols (Ng et al., 2011a; Fröhlich et al., 2013).
21 Aerosol sources have been successfully identified from the AMS measurements with positive matrix
22 factorization (PMF) analysis (Ulbrich et al., 2009; Crippa et al., 2013; Elser et al., 2016a). In terms of
23 Q-ACSM datasets, the use of PMF often fails to resolve sources with similar mass spectral profiles,
24 e.g. the mixing of cooking organic aerosol with traffic organic aerosol in Nanjing (Zhang et al.,
25 2015b); or those present in low contributions, e.g. the lack of success in resolving a factor related to
26 biomass burning in Beijing (Jiang et al., 2015). It was also pointed out that PMF cannot separate the
27 aerosol sources of temporal covariations driven by low temperature and periods of strong inversions

1 (Canonaco et al., 2013; Reyes et al., 2016). Several source apportionment studies (in which PMF did
2 not find optimal results) have utilized the multilinear engine (ME-2) solver, which enables constraint
3 of the factor profiles/time series, providing a superior separation of the PM sources ~~in Europe~~ (e.g.,
4 Canonaco et al., 2013; Canonaco et al., 2015; Fröhlich et al., 2015a; Fröhlich et al., 2015b;
5 Minguillón et al., 2015; Petit et al., 2015; Ripoll et al., 2015; Reyes et al., 2016; Bressi et al., 2016;
6 Schlag et al., 2016; [Wang et al., 2017](#); [Zhu et al., 2018](#)). However, studies using ME-2 to resolve OA
7 sources from the ACSM measurements are scarce in the BTH region.

8 Apart from the lack of applications of ME-2 for the OA source apportionment, most of the field
9 studies have mainly focused on the aerosol pollution in Beijing (Sun et al., 2013; Sun et al., 2014; Sun
10 et al., 2016; Jiang et al., 2015; Xu et al., 2015; Elser et al., 2016b; Hu et al., 2016a). These and related
11 studies have clearly shown that Beijing is sensitive to the regional transport of aerosols from its
12 surrounding areas (Xu et al., 2008; Zhang et al., 2012; Li et al., 2015a). For example, Guo et al.
13 (2010) estimated that the regional pollutants on average accounted for 69% of PM₁₀ and 87% of PM_{1,8}
14 in Beijing during summer, with sulfate, ammonium, and oxalate mostly formed regionally (regional
15 contributions >87%). Sun et al. (2014) reported that 66% of NR-PM₁ was from regional transport in
16 Beijing during the 2013 winter haze event. Among the surrounding areas of Beijing, the Hebei
17 province is the main source area leading to high aerosol loadings in Beijing (Chen et al., 2007; Xu et
18 al., 2008; Lang et al., 2013; Li et al., 2015a).

19 Shijiazhuang, the capital of Hebei province, is located ~270 km south of Beijing and has a population
20 approximately half that of Beijing. Zhao et al. (2013a, b) characterized the spatial and seasonal
21 variations of PM_{2.5} chemical composition in the BTH region, and Shijiazhuang was selected as the
22 representative of the polluted cities in Hebei province. The off-line analysis results showed that
23 organic carbon (OC) and elemental carbon (EC) concentrations in Shijiazhuang were lower in the
24 spring and summer than those in the autumn and winter. The sum of secondary inorganic species
25 (SO₄²⁻, NO₃⁻, and NH₄⁺) was highest in the autumn. Yet the temporal profiles of PM composition
26 cannot be captured by off-line analyses, hindering more detailed study on the sources and formation
27 of PM. In this work, we present for the first time the 30-minute time resolved NR-PM₁ measurements

1 in Shijiazhuang during the winter heating season. The characteristics of NR-PM₁ are analyzed, which
2 include (1) time series, mass fraction and diurnal variation of NR-PM₁ species; (2) multilinear engine
3 (ME-2)-resolved OA sources and their mass fraction as well as their diurnal variation; and (3) the
4 characteristics and atmospheric evolution of aerosol composition and sources under different aerosol
5 loadings and meteorological conditions.

6 **2 Methods**

7 **2.1 Sampling site**

8 Shijiazhuang, the capital of Hebei province, is located ~270 km south of Beijing. In 2014, ~10 million
9 residents and 2.1 million vehicles were reported in this city. It is often ranked the first in the list of top
10 10 most polluted cities in China, especially during wintertime heating periods (from 15 November to
11 15 March of the next year). For example, the average concentration of PM_{2.5} was 226.5 μg m⁻³ with
12 the peak hourly concentration of 933 μg m⁻³ during the 2013-2014 wintertime heating period, largely
13 exceeding the Chinese air pollution limit of 75 μg m⁻³. In this study, we performed an intensive field
14 measurement campaign at an urban site in Shijiazhuang to investigate the chemical composition,
15 sources and atmospheric processes of fine particles. The campaign was carried out from 11 January to
16 18 February 2014 on the building roof (15 m) of the Institute of Genetics and Developmental Biology,
17 Chinese Academy of Sciences (38°2'3''N, 114°32'29''E), a site located in a residential-business
18 mixed zone.

19 **2.2 Instrumentation**

20 NR-PM₁ was measured with an Aerodyne quadrupole aerosol chemical speciation monitor (Q-
21 ACSM), which can provide quantitative mass concentration and mass spectra of non-refractory
22 species including organics, sulfate, nitrate, ammonium, and chloride. The operation principles of Q-
23 ACSM can be found elsewhere (Ng et al., 2011a). The ambient aerosol was drawn through a Nafion
24 dryer (Perma Pure PD-50T-24SS) following a URG cyclone (Model: URG-2000-30ED) with a cut-off
25 size of 2.5 μm to remove coarse particles. The sampling flow was ~3 L min⁻¹, of which ~85 mL min⁻¹
26 was isokinetically sampled into the Q-ACSM. The residence time in the sampling tube was ~5 s. The
27 Q-ACSM was operated with a time resolution of 30 min and scanned from *m/z* 10 to 150 at 200 ms

1 amu⁻¹. Dry mono-dispersed 300-nm ammonium nitrate and ammonium sulfate particles (selected by a
2 differential mobility analyzer, DMA, TSI model 3080) were nebulized from a custom-built atomizer
3 and sampled into the Q-ACSM and a condensation particle counter (CPC, TSI model 3772)
4 calibrating ionization efficiency (IE). IE can, therefore, be determined by comparing the response
5 factors of Q-ACSM to the mass calculated with the known particle size and the number concentration
6 from CPC.

7 Ozone (O₃) was measured by a Thermo Scientific Model 49i ozone analyzer, CO by a Thermo
8 Scientific Model 48i carbon monoxide analyzer, SO₂ by an Ecotech EC 9850 sulfur dioxide analyzer,
9 and NO₂ by a Thermo Scientific Model 42i NO-NO₂-NO_x analyzer. The meteorological data,
10 including temperature, relative humidity (RH), precipitation, wind speed and wind direction, were
11 measured by an automatic weather station (MAWS201, Vaisala, Vantaa, Finland) and a wind sensor
12 (Vaisala Model QMW101-M2).

13 **2.3 Data analysis**

14 **2.3.1 Q-ACSM data analysis**

15 The mass concentrations and composition of NR-PM₁ were analyzed with the standard Q-ACSM data
16 analysis software written in Igor Pro (WaveMetrics, Inc., OR, USA). Standard relative ionization
17 efficiencies (RIEs) were used for organics, nitrate and chloride (i.e., 1.4 for organics, 1.1 for nitrate
18 and 1.3 for chloride) (Ng et al., 2011a) and RIEs for ammonium (6.0) and sulfate (1.2) were derived
19 from the IE calibrations. The particle collection efficiency (CE) was applied to correct for the particle
20 loss at the vaporizer due to particle bounce, which is influenced by aerosol acidity, composition, and
21 the aerosol water content. Given that aerosol was dried before entering into Q-ACSM and that
22 ammonium nitrate mass fraction (ANMF) during the observation period was lower than 0.4, the
23 composition dependent CE was estimated following the method described in Middlebrook et al.
24 (2012).

2.3.2 The Multilinear Engine (ME-2)

PMF is a bilinear receptor model that represents an input data matrix as a linear combination of a set of factor profiles and their time-dependent concentrations (Paatero and Tapper, 1994). Factors typically correspond to unique sources and/or processes. This allows for a quantitative apportionment of bulk mass spectral time series into several factors through the minimization of a quantity Q , which is the sum of the squares of the error-weighted residuals of the model. The PMF-AMS/ACSM analyses have been widely used for apportioning the sources of organic aerosol. However, in conventional PMF analyses, rotational ambiguity with limited rotational controls can lead to unclear factor resolution, especially in China where the emission sources are very complex and covariant during haze events. In contrast, the multi-linear engine (ME-2), used in this study, enables efficient exploration of the entire solution space and can direct the apportionment towards an environmentally-meaningful solution through the constraints of a subset of priori factor profiles or time series using the a value approach (Canonaco et al., 2013). The a value can vary between 0 and 1. An a value of 0.1 accounts for maximum $\pm 10\%$ variability of each m/z signal of the final solution spectra that may differ from the anchor, implying that some m/z signals might increase while some might decrease.

The source finder (SoFi, Canonaco et al., 2013) tool version 4.9 for Igor Pro was used for ME-2 input preparation and result analysis. The number of factors resolved is determined by the user and the solutions of the model are not mathematically unique due to rotational ambiguity. It is, therefore, critical to study other parameters, e.g., the chemical fingerprint of the factor profiles, diurnal cycles, and time series of factors and external measurements, to support factor identification and interpretation (Canonaco et al., 2013; Crippa et al., 2014, Elser et al., 2016b).

3 Results and discussion

3.1 Concentration and chemical composition of NR-PM₁

Fig. 1 shows the time series of NR-PM₁ species, trace gases and meteorological conditions during the entire measurement period. The measured mass concentrations of NR-PM₁ for the entire campaign period ranged from a few $\mu\text{g m}^{-3}$ to $508.4 \mu\text{g m}^{-3}$, with an average of $178 \pm 101 \mu\text{g m}^{-3}$. That was much higher than the wintertime/summertime concentrations measured in many other cities (see

1 Table 1). The mass concentration of NR-PM₁ correlated strongly with that of PM_{2.5} ($R^2 = 0.76$) with a
2 regression slope of 0.72, indicating that NR-PM₁ represents a majority of PM_{2.5} mass. The NR-PM₁
3 concentrations exceeded the Chinese PM_{2.5} limit of 75 $\mu\text{g m}^{-3}$ for 90% of days during the
4 measurement period, showing the severity of particulate air pollution at Shijiazhuang.

5 Similar to measurements at other urban sites, OA was the dominant fraction of NR-PM₁, with an
6 average of 50% (31-80%), followed by 21% of sulfate (4-36%), 12% of nitrate (2-26%), 11% of
7 ammonium (4-21%) and 6% of chloride (2-20%). The dominant contribution of organics in NR-PM₁
8 is also consistent with measurements from other urban sites in the BTH region during winter heating
9 seasons (see Table 1). Sulfate was the second largest contributor to NR-PM₁. The large fraction of
10 sulfate was likely associated with the large consumption of coal in Hebei province, i.e., 296 million
11 tons in 2014 were used in coal-fired power plants and steel industry (producing ~11% of global steel
12 output in 2014). The enhancement of chloride fraction from >1-4% in other Chinese cities in summer
13 (see Table 1) to 6% in Shijiazhuang in winter (within the range of >2-7% in other Chinese cities in
14 winter, see Table 1) can be attributed to the substantial emissions from coal and/or biomass burning
15 activities.

16 Fig. 2a shows the diurnal variations of NR-PM₁ components, which were affected by the evolution of
17 the planetary boundary layer (PBL) height that governed the vertical dispersion of pollutants and by
18 the diurnal cycle of the emissions and atmospheric processes. The concentrations of pollutants
19 increased at night as a result of enhanced emissions from residential heating (in particular, for
20 organics and chloride) and a progressively shallower PBL. During daytime the PBL height was
21 developed by solar radiation and thus the pollutants became diluted resulting in the decrease of
22 organics, sulfate, ammonium and chloride in the afternoon. In contrast, the concentrations of nitrate
23 increased after sunrise but then kept rather constant throughout the afternoon, suggesting a strong
24 source or production of nitrate which offsets the dilution from PBL development. To minimize the
25 effects from PBL heights, data were normalized by ΔCO . CO is often used as an emission tracer to
26 account for dilution on timescales of hours to days because of its relatively long life time against the
27 oxidation by OH radicals (approximately one month) (Decarlo et al., 2010). After offsetting the PBL

1 dilution effect, sulfate, nitrate and ammonium showed clear increases from 7:00 to 15:00 (Fig. 2c),
2 indicating efficient daytime production of these secondary inorganic species. It should be noted that
3 the increase of nitrate (about 2 times, from $\sim 6 \mu\text{g m}^{-3} \text{ppm}^{-1}$ to $\sim 12 \mu\text{g m}^{-3} \text{ppm}^{-1}$) is slightly larger
4 than that of sulfate (about 1.6 times, from $\sim 11 \mu\text{g m}^{-3} \text{ppm}^{-1}$ to $\sim 17.5 \mu\text{g m}^{-3} \text{ppm}^{-1}$), indicating more
5 efficient photochemical production of nitrate than sulfate, given that the loss rate of sulfate could not
6 be higher than that of nitrate as nitric acid is semi-volatile and may be further lost by evaporation.
7 Also, the continuous increase of organics after sunrise suggested efficient photochemical production
8 of secondary organic aerosol (SOA).

9 **3.2 Sources of organic aerosol**

10 From the PMF analysis, we first examined a range of solutions with 3 to 8 factors. The solution that
11 best represents the data is the 5-factor solution (Fig. S1). The solutions with factor numbers more than
12 5 provide no new meaningful factors (see Fig. S2 and more details in the supplementary material).

13 Although the 5-factor solution can reasonably represent the data, HOA is still mixed with BBOA
14 because the HOA profile contains higher than expected contribution from m/z 60. In addition, COA
15 contains no signal at m/z 44, which might indicate a suboptimal splitting between the contributing
16 sources. To better separate HOA from BBOA, we constrained the HOA profile from Ng et al (2011b),
17 which is an average profile over 15 cities from China, Japan, Europe and the United States. Although
18 gasoline vehicles dominate in China while diesel vehicles dominate in Europe, HOA mass spectra do
19 not show significant variability when compared to different sites in China and Europe (Ng et al.,
20 2011b; Reyes et al., 2016; Bozzetti et al., 2017), indicating that traffic emissions from different types
21 of vehicles have similar profiles. To avoid the influences of other sources on COA, the COA profile
22 from Paris (Crippa et al., 2013) was used as a constraint because high similarities were found between
23 the COA profile from Paris and four COA profiles from different types of Chinese cooking activities
24 (He et al., 2010; Crippa et al., 2013). However, the constraint on HOA and COA profiles still seems
25 to sub-optimally resolve the apportionment of BBOA from CCOA, as one unconstrained factor
26 contains high contributions from both m/z 60 and PAH-related m/z 's (m/z 77, 91 and 115, as shown in
27 Fig. S3) which indicate the mixing between BBOA and CCOA. To separate BBOA and CCOA, we

1 constrained BBOA using the average of BBOA profiles from the 5-factor unconstrained PMF
2 solutions.

3 To explore the solution space, a value of 0-0.5 with an interval of 0.1 was used to constrain both the
4 HOA and COA reference profiles from literature while BBOA was constrained with a value of 0
5 because the BBOA profile was resolved from unconstrained PMF solution which is not expected to
6 vary significantly. 36 possible results were obtained by limiting a range of a values. Three criteria for
7 optimizing OA source appointment are as follows:

8 (1) *The diurnal pattern of COA.* The diurnal cycle of COA should have higher concentrations
9 during mealtime.

10 (2) *Minimization of m/z 60 in HOA.* The upper limit of m/z 60 in the HOA profile is 0.006, which
11 is the maximal fractional contribution derived from multiple ambient data sets in different
12 regions (mean + 2σ) (Ng et al., 2011b).

13 (3) *The rationality of unconstrained factors.* OOA should have abundant signal at m/z 44 and
14 contain much lower signals at PAH-related ion peaks compared to CCOA.

15 Nine solutions match the criteria above. The final time series and mass spectra are therefore the
16 averages of these 9 solutions. The diurnal variations of mass concentrations of the OA factors and
17 their PBL-corrected results are shown in Fig. 2b and d, respectively. The mass spectra and time series
18 of the OA factors and their correlation with external tracers are shown in Fig. 3. The relative
19 contributions of each OA source to the m/z 's are shown in Fig. S4. Potential source contribution
20 function (PSCF) analysis was also performed and the result is shown in Fig. S5.

21 OOA is characterized by high signals at m/z 44 (CO_2^+) and m/z 43 (C_3H_7^+ or $\text{C}_2\text{H}_3\text{O}^+$). OOA accounts
22 for 85% of m/z 44 signal, much higher than other OA sources. The time series of OOA is highly
23 correlated with that of sulfate ($R^2=0.70$), nitrate ($R^2=0.75$) and ammonium ($R^2=0.76$), confirming the
24 secondary nature of this factor. The diurnal cycle of OOA shows an increase from 7:00 to 11:00,
25 followed by a decrease in the afternoon due to the PBL evolution effect. After normalizing the PBL
26 effect, OOA increased continuously from 7:00 to 15:00, indicating the importance of photochemical

1 oxidation. This diurnal feature together with the PSCF results indicated that a large fraction of OOA
2 was produced locally and/or produced from the highly populated and industrialized surrounding areas,
3 consistent with the sulfate production discussed below.

4 The mass spectrum of CCOA is featured by prominent contributions of unsaturated hydrocarbons,
5 particularly PAH-related ion peaks (e.g., 77, 91, and 115). The CCOA profile shows a weaker signal
6 at m/z 44 than that observed in Beijing (Hu et al., 2016a) and Lanzhou (Xu et al., 2016). This
7 difference can be caused by the difference in coal types, burning conditions and aging processes
8 (Zhou et al., 2016). CCOA accounts for 42-66% of PAH-related ion peaks, much higher than those in
9 other OA sources. This result suggested that the major source of PAHs was coal combustion in
10 wintertime Shijiazhuang. The campaign-averaged mass concentration of CCOA was $23.2 \mu\text{g m}^{-3}$,
11 which is higher than that in Xi'an ($10.1 \mu\text{g m}^{-3}$) but is similar to that in Beijing ($23.5 \mu\text{g m}^{-3}$) observed
12 in the same winter (Elser et al., 2016a). Nevertheless, during haze extremes, the average CCOA
13 concentration was $77.5 \mu\text{g m}^{-3}$ in Shijiazhuang, much higher than that in Beijing ($48.2 \mu\text{g m}^{-3}$, Elser et
14 al., 2016a). CCOA showed distinct diurnal variations with low concentration down to $12.6 \mu\text{g m}^{-3}$
15 during the day and high concentration up to $37.6 \mu\text{g m}^{-3}$ at night, corresponding to 19% and 35% of
16 OA, respectively. The elevated CCOA concentrations at night suggested a large emission from
17 residential heating activities using coal as the fuel compounded by the shallow PBL. The average
18 contribution of CCOA to the total OA was 27%, which is consistent with studies in Beijing and
19 Handan (~160 km south to Shijiazhuang) where CCOA was found to be the dominant primary OA
20 (Elser et al., 2016a; Sun et al., 2016; Li et al., 2017). Given this large fraction of OA from coal
21 combustion, mitigating residential coal combustion is therefore of significant importance for
22 improving air quality in the BTH regions.

23 The BBOA mass spectrum is featured by prominent m/z 60 (mainly $\text{C}_2\text{H}_4\text{O}_2^+$) and 73 (mainly
24 $\text{C}_3\text{H}_5\text{O}_2^+$) signals (He et al., 2010). These two ions ($\text{C}_2\text{H}_4\text{O}_2^+$ and $\text{C}_3\text{H}_5\text{O}_2^+$) are fragments of
25 anhydrous sugars produced from the incomplete combustion and pyrolysis of cellulose and
26 hemicelluloses (Alfarra et al., 2007; Lanz et al., 2007; Mohr et al., 2009). Consistently, BBOA
27 accounts for 50% of m/z 60 and 56% of m/z 73, much higher than those in other sources. In addition,

1 BBOA accounts for 9-27% of the PAH-related m/z 's (i.e., m/z 77, 91 and 115), lower than that in
2 CCOA but higher than those in other primary OA sources. This suggested that BBOA was also an
3 important PAH source in wintertime Shijiazhuang. A high correlation was found between the time
4 series of BBOA and that of chloride ($R^2=0.75$), the latter of which was suggested to be one of the
5 tracers of biomass burning. BBOA on average accounted for 17% of OA, which is higher than those
6 (9-12%) observed in Beijing during wintertime heating seasons (Elser et al., 2016a; Hu et al., 2016a;
7 Sun et al., 2016). The higher BBOA contribution in wintertime Shijiazhuang is likely associated with
8 widespread use of wood and crop residuals for heating and cooking in Shijiazhuang and surrounding
9 areas, as supported by the PSCF results (Fig. S5).

10 The COA profile is characterized by a high m/z 55/57 ratio of 2.7, much higher than that in non-
11 cooking POA (0.6-1.1) but within the range of 2.2-2.8 in COA profiles reported by Mohr et al.
12 (2012). COA shows a clear diurnal cycle with distinct peaks at lunch (between 11:00-13:00 local
13 time, LT) and dinner (between 19:00-21:00 LT) times. A small peak was also observed in the
14 morning between 06:00 and 07:00 LT, consistent with the breakfast time. COA on average accounted
15 for 16% of total OA with the highest contribution of 24% during dinner time.

16 The HOA mass spectrum is dominated by hydrocarbon ion series of $[C_nH_{2n+1}]^+$ and $[C_nH_{2n-1}]^+$
17 (Canagaratna et al., 2004; Mohr et al., 2009). The diurnal variation of HOA is featured by high
18 concentration at night, likely due to enhanced truck emissions (only allowed to drive on road from
19 23:00 to 6:00 LT) and shallow PBL at night. Similar diurnal cycles were found in wintertime Beijing
20 and Xi'an (Sun et al., 2016; Elser et al., 2016a). HOA, on average, accounted for 13% of total OA for
21 the entire observation period, which was higher than that in Beijing (9-10%) but lower than that in
22 Xi'an (15%) measured in the same winter (Elser et al., 2016a; Sun et al., 2016).

23 **3.3 Chemical nature and sources at different PM levels**

24 Fig. 4 shows the mass fractions of NR-PM₁ species and OA sources on reference days and extremely
25 polluted days. Here, the days with NR-PM₁ daily average mass concentration higher than the 75th
26 percentile (i.e., $\geq 238 \mu\text{g m}^{-3}$) are denoted as the extremely polluted days and the rest of days as
27 reference days. The average concentration of NR-PM₁ was $310 \mu\text{g m}^{-3}$ during extremely polluted

1 days, about 2 times higher than that during reference days ($162 \mu\text{g m}^{-3}$). The average concentration of
2 secondary inorganic aerosol was $65 \mu\text{g m}^{-3}$ (40% of NR-PM₁ mass) during reference days and
3 increased to $143 \mu\text{g m}^{-3}$ (46% of NR-PM₁ mass) during extremely polluted days. Secondary organic
4 aerosol also increased from $19 \mu\text{g m}^{-3}$ (22% of OA) during reference days to $40 \mu\text{g m}^{-3}$ (26% of OA)
5 during extremely polluted days. The enhanced mass concentrations (~ 2 times) of both secondary
6 inorganic aerosol and secondary organic aerosol during extremely pollution days suggested strong
7 secondary aerosol production during pollution events. Such enhancement was likely
8 ~~confounded~~ compounded by stagnant weather conditions (e.g., average wind speed was 0.9 m s^{-1}) and
9 high RH of 69.4% which facilitated the production and accumulation of secondary aerosol. Note that
10 it was already very polluted during the reference days with an average concentration of NR-PM₁ of
11 $162 \mu\text{g m}^{-3}$, which may explain the relatively small increase in fractional contribution of secondary
12 aerosol from reference days to extremely polluted days.

13 Fig. 5a and b show the factors driving the pollution events by binning the fractional contribution of
14 each chemical species and OA source to total NR-PM₁ and OA mass, respectively. The data clearly
15 show that high pollution events are characterized by an increasing secondary fraction, reaching $\sim 55\%$
16 at the highest NR-PM₁ mass bin ($300\text{-}360 \mu\text{g m}^{-3}$). In particular, from the lowest NR-PM₁ bin to the
17 highest NR-PM₁ bin, the fractional contribution increases from 14% to 25% for sulfate in NR-PM₁
18 and from 18% to 25% for OOA in OA, demonstrating the importance of secondary aerosol formation
19 in driving particulate air pollution (Huang et al., 2014; Elser et al., 2016; Wang et al., 2017). To
20 investigate the oxidation degree of sulfur at different NR-PM₁ mass, the sulfur oxidation ratio (F_{SO_4})
21 was calculated according to Eq. (1)

$$F_{\text{SO}_4^{2-}} = \frac{n[\text{SO}_4^{2-}]}{n[\text{SO}_4^{2-}] + n[\text{SO}_2]} \quad (1)$$

22
23 where n is the molar concentration. As can be seen from Fig. 6, F_{SO_4} shows a clear increase trend with
24 NR-PM₁ mass, increasing from 0.08 in the lowest mass bin to 0.21 in the highest mass bin. However,
25 the highest F_{SO_4} value is still much lower than that reported in previous studies, e.g., 0.62 in Xi'an

1 (Elser et al., 2016), suggesting low atmospheric oxidative capacity during the measurement period in
2 Shijiazhuang. This may also explain the relatively low OOA fraction (see Fig. 5b). Certainly, it
3 should be noted that the mass concentration of sulfate may also be affected by other parameters
4 including aerosol liquid water content, aerosol or cloud water pH, besides atmospheric oxidative
5 capacity.

6 **3.4 Evolution of aerosol composition and sources at different RH levels**

7 Fig. 7a and b show the mass concentrations of the NR-PM₁ species and of the OA sources as a
8 function of RH, with RH bins of 10% increments. The absolute mass concentrations of secondary
9 inorganic species increased as RH increased from ~~<60% to 90%~~ 60%, while chloride showed a
10 decreasing trend. Among the OA sources, OOA and HOA ~~were~~ significantly enhanced with RH
11 increasing from <60% to 90%, while other OA sources did not show a clear trend. As RH increased
12 gradually with the decrease of wind speed (Fig. 6a), the development of stagnant weather conditions
13 (including a shallower PBL) promoted both the accumulation of pollutants and the formation of
14 secondary aerosol (Tie et al., 2016). To minimize the effects from PBL variations, the NR-PM₁
15 species and OA fractions were normalized by the sum of the POA, as a surrogate of secondary aerosol
16 precursors. The resulting ratios were further normalized by the values at the first RH bin (<60%) for
17 better visualization. As shown in Fig. 7c, when RH increased from ~~<60% to >90%~~ 60% to 100%, the
18 normalized sulfate increased by a factor of ~ 1.72 ~~1.5~~, suggesting the importance of aqueous-phase SO₂
19 oxidation in the formation of sulfate at high RH. The enhancements for nitrate and ammonium were
20 slightly lower (~ 1.2 ~~1.5~~) compared to that sulfate, because NH₄NO₃ is thermally labile and its gas-
21 particle partitioning is affected by both temperature and RH. The importance of aqueous-phase
22 chemistry is further supported by the increase of F_{SO_4} as a function of RH (Fig. 6b). At RH <60%,
23 F_{SO_4} was rather constant, with an average of 0.09, indicating a low sulfur oxidation degree. At
24 RH >60%, F_{SO_4} increased rapidly with the increase of RH, reaching a maximal average of 0.18 at the
25 last RH bin (90-100%). Note that the sulfur oxidation degree at high RH (>60%) was much lower
26 compared to those measured in Xi'an during the same winter (average F_{SO_4} 0.62 at RH=90-100%,
27 Elser et al., 2016a). The low sulfur oxidation degree observed in Shijiazhuang (i.e., >80% of sulfur is

1 still not oxidized) indicated insufficient atmospheric processing and also suggested a large fraction of
2 pollutants in Shijiazhuang was likely emitted locally and/or transported from the heavily populated
3 and industrialized surrounding areas. With a longer atmospheric processing time in the downwind
4 region, e.g., Beijing, higher secondary aerosol fractions are expected, as observed in previous studies
5 (e.g., Huang et al., 2014). Similar to sulfate, the normalized OOA increased by a factor of ~ 1.23
6 when RH increased from ~~<60%~~ 60% to ~~90~~-100% (Fig. 7d). The mass fraction of OOA increased from
7 29% to 41% when RH increased from 70% to 100%, while POA contribution decreased
8 correspondingly from 71% to 59% (Fig. 6d). These results support the above discussion that aqueous-
9 phase chemistry also plays an important role in the formation of OOA under high RH conditions
10 during haze pollution episodes.

11 **3.5 Primary emissions versus secondary formation**

12 Frequent changes between clean and polluted episodes were observed in this study. To get a better
13 insight into aerosol sources and atmospheric processes, 4 clean periods (C1-C4) with daily average
14 mass concentration of NR-PM₁ lower than the 25th percentile, 6 high-RH (>80%) polluted episodes
15 (H1-H6) and 4 low-RH (<60%) polluted episodes (L1-L4) with daily average mass concentration of
16 NR-PM₁ higher than the 75th percentile were selected for further analysis. As shown in the Fig. 8, the
17 chemical composition and sources differed during different episodes. The contributions of organics
18 showed a decreasing trend, from 54-64% during C1-C4 to 49-58% during L1-L4, and to 35-44%
19 during H1-H6, while the corresponding contributions of secondary inorganic species increased. This
20 indicated a notable production and accumulation of secondary inorganic aerosol during severe haze
21 pollution events. For example, the mass fraction of sulfate in NR-PM₁ was much higher during high
22 RH pollution events (H1-H6, 27-30%) compared to those during low RH pollution events (L1-L4, 11-
23 18%) and clean events (C1-C4, 11-17%). OOA also showed a much higher contribution to OA during
24 high RH pollution events (H1-H6, 29-50%) than during low RH pollution events (L1-L3, 17-26%)
25 and clean events (C1-C4, 10-34%). Interestingly, when comparing high RH and low RH pollution
26 events of similar PM levels (Fig. 8), secondary inorganic species and OOA dominated the particulate
27 pollution at high RH pollution events likely due to enhanced secondary formation, similar to previous

1 studies (e.g., Wang et al., 2017), while POA dominated the particulate pollution at low RH and under
2 stagnant conditions. The concentrations of POA are determined by both emissions and meteorological
3 conditions. The different significance of primary aerosol and secondary aerosol in low and high RH
4 pollution events highlights ~~These results highlight~~ the importance of meteorological conditions in
5 driving particulate pollution.

6 Fig. 9 shows the evolution of aerosol species in two cases of different RH levels. The first case had
7 average RH <50% from 20-24 Jan (C2 and L3 episodes). The high wind speed (>6 m s⁻¹) from the
8 northwest before the L3 episode led to a significant reduction of air pollutants (the C3 episode, a
9 clean-up period). When the wind direction switched from northwest to 90°-270° sector and the wind
10 speed decreased to <3 m s⁻¹, the measured pollutants (except O₃ which was reacted out by increasing
11 NO emissions) started to build up. Specifically, NR-PM₁ showed a dramatic increase by a factor of 19
12 over the first 11 hours (from 20 Jan 16:00 to 21 Jan 3:00 LT) from 12 to 233 μg m⁻³. In this process
13 POA contributed to an average 69% of NR-PM₁ mass. The other three processes were also
14 characterized by a rapid increase of NR-PM₁ mass (39-50 μg m⁻³ h⁻¹) and high contribution of POA,
15 i.e., from 22 Jan 0:00-22 Jan 3:00, 22 Jan 16:00-22 Jan 20:00, and 23 Jan 12:00-23 Jan 19:00. Such
16 rapid increases in NR-PM₁ mass under low RH were associated with stagnant weather conditions
17 (e.g., low wind speed) which promoted the accumulation of pollutants. The second case had average
18 RH >80% from 5-8 Feb (H3 and H4 episodes). In this case, the wind speed was low (<3 m s⁻¹)
19 throughout the 4-day period. Under this very stagnant weather condition, POA accumulated
20 continuously (Fig. 9). However, different from the low-RH case, the concentration of secondary
21 species also showed continuous increases in this high-RH case. The enhancement of secondary
22 aerosol formation was likely driven by aqueous-phase chemistry at high RH level (Elser et al., 2016;
23 Wang et al., 2017) and the accumulation of pollutants under stagnant weather conditions (Tie et al.,
24 2017) which further promoted the formation of secondary species.

25 **4 Conclusions**

26 ~~A Quadrupole Aerosol Chemical Speciation Monitor (Q-ACSM) was deployed in Shijiazhuang from~~
27 ~~11 January to 18 February 2014 to investigate the~~ The chemical nature, sources and atmospheric

1 processes of wintertime fine particles in Shijiazhuang were investigated, in this heavily polluted city.
2 ~~The average mass concentration of NR-PM₁ was 178 ± 101 μg m⁻³, much higher than the wintertime~~
3 ~~concentrations measured in many other cities. Organics were the dominant composition (50%),~~
4 ~~followed by sulfate (21%), nitrate (12%), ammonium (11%) and chloride (6%). As for the sources of~~
5 ~~OA, OOA (27%) and CCOA (27%) were on average the most abundant sources, followed by BBOA~~
6 ~~(17%), COA (16%) and HOA (13%).~~ The mass fractions of secondary inorganic species and SOA
7 increased with the increase of NR-PM₁ mass, suggesting the importance of secondary formation in
8 driving PM pollution. However, the low sulfur oxidation degree and low OOA fraction indicated
9 insufficient atmospheric oxidation capacity. Together with the diurnal variations and PSCF results,
10 these observations suggested that a large fraction of pollutants in Shijiazhuang was most likely
11 produced locally and/or transported from the heavily populated and industrialized surrounding areas
12 without sufficient atmospheric aging. Two different regimes were found to be responsible for the high
13 PM pollution in Shijiazhuang. At low RH under stagnant weather conditions, the accumulation of
14 primary emissions was the main culprit. In contrast, at high RH, the enhanced formation of secondary
15 aerosol through aqueous-phase chemistry was the main culprit. To conclude, we found that in this
16 highly polluted city in North China, (1) secondary formation is important in high-PM episodes, (2)
17 primary emissions are still important on an average basis, and (3) meteorological conditions play an
18 important part in pollutant accumulation and transformation. The findings from this study thus
19 suggest that (a) there are still opportunities for air pollution mitigation by controlling direct emissions
20 such as coal combustion, and (b) control on precursors (e.g., NO_x, SO₂, and VOCs) for secondary
21 formation, especially during high-PM episodes with unfavorable meteorological conditions, can ease
22 the situation substantially.

23 **5 Acknowledgement**

24 This research is supported by the National Science Foundation of China (No. 91644219, [41877408](#),
25 and 41675120), and EPA-Ireland (AEROSOURCE, 2016-CCRP-MS-31).

26

1 **References**

- 2 Alfarra, M. R., Prévôt, A. S. H., Szidat, S., Sandradewi, J., Weimer, S., Schreiber, D., Mohr, M., and
3 Baltensperger, U.: Identification of the mass spectral signature of organic aerosols from wood burning
4 emissions, *Environ. Sci. Technol.*, 41, 5770–5777, 2007.
- 5 Bozzetti, C., El Haddad, I., Salameh, D., Daellenbach, K. R., Fermo, P., Gonzalez, R., Minguillón, M.
6 C., Iinuma, Y., Poulain, L., Müller, E., Slowik, J. G., Jaffrezo, J.-L., Baltensperger, U., Marchand, N.,
7 and Prévôt, A. S. H.: Organic aerosol source apportionment by offline-AMS over a full year in
8 Marseille, *Atmos. Chem. Phys. Discuss.*, 17, 8247-8268, 2017.
- 9 Bressi, M., Cavalli, F., Belis, C. A., Putaud, J.-P., Fröhlich, R., Martins dos Santos, S., Petralia, E.,
10 Prévôt, A. S. H., Berico, M., Malaguti, A., and Canonaco, F.: Variations in the chemical composition
11 of the submicron aerosol and in the sources of the organic fraction at a regional background site of the
12 Po Valley (Italy), *Atmos. Chem. Phys.*, 16, 12875-12896, <https://doi.org/10.5194/acp-16-12875-2016>,
13 2016.
- 14 Canagaratna, M. R., Jayne, J. T., Ghertner, D. A., Herndon, S., Shi, Q., Jimenez, J. L., Silva, P. J.,
15 Williams, P., Lanni, T., Drewnick, F., Demerjian, K. L., Kolb, C. E., Worsnop, D. R.: Chase studies
16 of particulate emissions from in-use New York City vehicles, *Aerosol Sci. Tech.* 38, 555-573, 2004.
- 17 Canonaco, F., Crippa, M., Slowik, J. G., Baltensperger, U., and Prévôt, A. S. H.: SoFi, an IGOR
18 based interface for the efficient use of the generalized multilinear engine (ME-2) for the source
19 apportionment: ME-2 application to aerosol mass spectrometer data, *Atmos. Meas. Tech.*, 6, 3649–
20 3661, doi:10.5194/amt-6-3649-2013, 2013.
- 21 Canonaco, F., Slowik, J. G., Baltensperger, U., and Prévôt, A. S. H.: Seasonal differences in
22 oxygenated organic aerosol composition: implications for emissions sources and factor analysis,
23 *Atmos. Chem. Phys.*, 15, 6993-7002, doi:10.5194/acp-15-6993-2015, 2015.
- 24 Chen, D. S., Cheng, S. Y., Liu, L., Chen, T., Guo, X. R.: An integrated MM5-CMAQ modeling
25 approach for assessing trans-boundary PM10 contribution to the host city of 2008 Olympic summer
26 games-Beijing, China, *Atmospheric Environment*, 41, 1237-1250, 2007.

1 [Cohen, A. J., Brauer, M., Burnett, R., Anderson, H. R., Frostad, J., Estep, K., Balakrishnan, K.,](#)
2 [Brunekreef, B., Dandona, L., Dandona, R., Feigin, V., Freedman, G., Hubbell, B., Jobling, A., Kan,](#)
3 [H. D., Knibbs, L., Liu, Y., Martin, R., Morawska, L., Pope III, C. A., Shin, H., Straif, K., Shaddick,](#)
4 [G., Thomas, M., van Dingenen, R., van Donkelaar, A., Vos, T., Murray, C. J. L., Forouzanfar, M. H.:](#)
5 [Estimates and 25-year trends of the global burden of disease attributable to ambient air pollution: an](#)
6 [analysis of data from the Global Burden of Diseases Study 2015. *The Lancet* 389, 1907-1918, 2017.](#)

7 Crippa, M., DeCarlo, P. F., Slowik, J. G., Mohr, C., Heringa, M. F., Chirico, R., Poulain, L., Freutel,
8 F., Sciare, J., Cozic, J., Di Marco, C. F., Elsasser, M., Nicolas, J. B., Marchand, N., Abidi, E.,
9 Wiedensohler, A., Drewnick, F., Schneider, J., Borrmann, S., Nemitz, E., Zimmermann, R., Jaffrezo,
10 J.-L., Prévôt, A. S. H., and Baltensperger, U.: Wintertime aerosol chemical composition and source
11 apportionment of the organic fraction in the metropolitan area of Paris, *Atmos. Chem. Phys.*, 13, 961-
12 981, doi:10.5194/acp-13-961-2013, 2013.

13 Crippa, M., Canonaco, F., Lanz, V. A., Äijälä, M., Allan, J. D., Carbone, S., Capes, G., Ceburnis, D.,
14 Dall'Osto, M., Day, D. A., DeCarlo, P. F., Ehn, M., Eriksson, A., Freney, E., Hildebrandt Ruiz, L.,
15 Hillamo, R., Jimenez, J. L., Junninen, H., Kiendler-Scharr, A., Kortelainen, A.-M., Kulmala, M.,
16 Laaksonen, A., Mensah, A. A., Mohr, C., Nemitz, E., O'Dowd, C., Ovadnevaite, J., Pandis, S. N.,
17 Petäjä, T., Poulain, L., Saarikoski, S., Sellegri, K., Swietlicki, E., Tiitta, P., Worsnop, D. R.,
18 Baltensperger, U., and Prévôt, A. S. H.: Organic aerosol components derived from 25 AMS data sets
19 across Europe using a consistent ME-2 based source apportionment approach, *Atmos. Chem. Phys.*,
20 14, 6159– 6176, doi:10.5194/acp-14-6159-2014, 2014.

21 Decarlo, P. F., Ulbrich, I. M., Crouse, J., De Foy, B., Dunlea, E. J., Aiken, A. C., Knapp, D.,
22 Weinheimer, A. J., Campos, T., Wennberg, P. O., Jimenez, J. L.: Investigation of the sources and
23 processing of organic aerosol over the Central Mexican Plateau from aircraft measurements during
24 MILAGRO, *Atmos. Chem. Phys.*, 10, 5257-5280, doi:10.5194/acp-10-5257-2010, 2010

25 Elser, M., Huang, R.-J., Wolf, R., Slowik, J. G., Wang, Q., Canonaco, F., Li, G., Bozzetti, C.,
26 Daellenbach, K. R., Huang, Y., Zhang, R., Li, Z., Cao, J., Baltensperger, U., El-Haddad, I., and
27 Prévôt, A. S. H.: New insights into PM_{2.5} chemical composition and sources in two major cities in

1 China during extreme haze events using aerosol mass spectrometry, *Atmos. Chem. Phys.*, 16, 3207-
2 3225, doi:10.5194/acp-16-3207-2016, 2016a.

3 Elser, M., Bozzetti, C., El-Haddad, I., Maasikmets, M., Teinemaa, E., Richter, R., Wolf, R., Slowik, J.
4 G., Baltensperger, U., and Prévôt, A. S. H.: Urban increments of gaseous and aerosol pollutants and
5 their sources using mobile aerosol mass spectrometry measurements, *Atmos. Chem. Phys.*, 16, 7117-
6 7134, doi:10.5194/acp-16-7117-2016, 2016b.

7 Ervens, B., Turpin, B. J., and Weber, R. J.: Secondary organic aerosol formation in cloud droplets and
8 aqueous particles (aqSOA): a review of laboratory, field and model studies, *Atmos. Chem. Phys.*, 11,
9 11069–11102, doi:10.5194/acp-11-11069-2011, 2011.

10 Fröhlich, R., Cubison, M. J., Slowik, J. G., Bukowiecki, N., Prévôt, A. S. H., Baltensperger, U.,
11 Schneider, J., Kimmel, J. R., Gonin, M., Rohner, U., Worsnop, D. R., and Jayne, J. T.: The ToF-
12 ACSM: a portable aerosol chemical speciation monitor with TOFMS detection, *Atmos. Meas. Tech.*,
13 6, 3225-3241, <https://doi.org/10.5194/amt-6-3225-2013>, 2013.

14 Fröhlich, R., Crenn, V., Setyan, A., Belis, C. A., Canonaco, F., Favez, O., Riffault, V., Slowik, J. G.,
15 Aas, W., Aijälä, M., Alastuey, A., Artiñano, B., Bonnaire, N., Bozzetti, C., Bressi, M., Carbone, C.,
16 Coz, E., Croteau, P. L., Cubison, M. J., Esser-Gietl, J. K., Green, D. C., Gros, V., Heikkinen, L.,
17 Herrmann, H., Jayne, J. T., Lunder, C. R., Minguillón, M. C., Mocnik, G., O’Dowd, C. D.,
18 Ovadnevaite, J., Petralia, E., Poulain, L., Priestman, M., Ripoll, A., Sarda-Estève, R., Wiedensohler,
19 A., Baltensperger, U., Sciare, J., and Prévôt, A. S. H.: ACTRIS ACSM intercomparison–Part 2:
20 Intercomparison of ME-2 organic source apportionment results from 15 individual, co-located aerosol
21 mass spectrometers, *Atmos. Meas. Tech.*, 8, 2555–2576, doi:10.5194/amt- 8-2555-2015, 2015a.

22 Fröhlich, R., Cubison, M. J., Slowik, J. G., Bukowiecki, N., Canonaco, F., Croteau, P. L., Gysel, M.,
23 Henne, S., Herrmann, E., Jayne, J. T., Steinbacher, M., Worsnop, D. R., Baltensperger, U., and
24 Prévôt, A. S. H.: Fourteen months of on-line measurements of the non-refractory submicron aerosol at
25 the Jungfraujoch (3580 m a.s.l.) – chemical composition, origins and organic aerosol sources, *Atmos.*
26 *Chem. Phys.*, 15, 11373-11398, doi:10.5194/acp-15-11373-2015, 2015b.

1 Ge, X., Zhang, Q., Sun, Y. L., Ruehl, C. R., and Setyan, A.: Effect of aqueous-phase processing on
2 aerosol chemistry and size distributions in Fresno, California, during wintertime, *Environmental*
3 *Chemistry*, 9, 221–235, doi:10.1071/EN11168, 2012.

4 Guo, S., Hu, M., Wang, Z. B., Slanina, J., and Zhao, Y. L.: Size resolved aerosol water-soluble ionic
5 compositions in the summer of Beijing: implication of regional secondary formation, *Atmos. Chem.*
6 *Phys.*, 10, 947–959, doi:10.5194/acp-10-947-2010, 2010.

7 He, L.-Y., Lin, Y., Huang, X.-F., Guo, S., Xue, L., Su, Q., Luan, S.- J., and Zhang, Y.-H.:
8 Characterization of high-resolution aerosol mass spectra of primary organic aerosol emissions from
9 Chinese cooking and biomass burning, *Atmos. Chem. Phys.*, 10, 11535– 11543, doi:10.5194/acp-10-
10 11535-2010, 2010.

11 He, L.-Y., Huang, X.-F., Xue, L., Hu, M., Lin, Y., Zheng, J., Zhang, R., and Zhang, Y.-H.: Submicron
12 aerosol analysis and organic source apportionment in an urban atmosphere in Pearl River Delta of
13 China using high-resolution aerosol mass spectrometry, *J. Geophys. Res.*, 116, D12304,
14 doi:10.1029/2010JD014566, 2011.

15 Hu, W., Hu, M., Hu, W., Jimenez, J. L., Yuan, B., Chen, W., Wang, M., Wu, Y., Chen, C., Wang, Z.,
16 Peng, J., Zeng, L., and Shao, M.: Chemical composition, sources and aging process of submicron
17 aerosols in Beijing: contrast between summer and winter, *J. Geophys. Res.*, 121, 1955–1977,
18 doi:10.1002/2015JD024020, 2016a.

19 Hu, W., Hu, M., Hu, W.-W., Niu, H., Zheng, J., Wu, Y., Chen, W., Chen, C., Li, L., Shao, M., Xie,
20 S., and Zhang, Y.: Characterization of submicron aerosols influenced by biomass burning at a site in
21 the Sichuan Basin, southwestern China, *Atmos. Chem. Phys.*, 16, 13213-13230, doi:10.5194/acp-16-
22 13213-2016, 2016b.

23 Huang, R. J., Zhang, Y., Bozzetti, C., Ho, K. F., Cao, J. J., Han, U., Daellenbach, K. R., Slowik, J. G.,
24 Platt, S. M., Canonaco, F., Zotter, P., Wolf, R., Pieber, S. M., Brun, E. A., Crippa, M., Ciarelli, G.,
25 Piazzalunga, A., Schwikowski, M., Abbaszade, G., Schnelle-Kreis, J., Zimmermann, R., An, Z.,

1 Szidat, S., Baltensperger, U., El Haddad, I. and Prévôt, A. S. H.: High secondary aerosol contribution
2 to particulate pollution during haze events in China, *Nature*, 514, 218–222, 2014.

3 Huang, X.-F., He, L.-Y., Xue, L., Sun, T.-L., Zeng, L.-W., Gong, Z.-H., Hu, M., and Zhu, T.: Highly
4 time-resolved chemical characterization of atmospheric fine particles during 2010 Shanghai World
5 Expo, *Atmos. Chem. Phys.*, 12, 4897-4907, doi:10.5194/acp-12-4897-2012, 2012.

6 Huang, X.-F., Xue, L., Tian, X.-D., Shao, W.-W., Sun, T.-L., Gong, Z.-H., Ju, W.-W., Jiang, B., Hu,
7 M., and He, L.-Y.: Highly time-resolved carbonaceous aerosol characterization in yangtze river delta
8 of china: Composition, mixing state and secondary formation, *Atmos. Environ.*, 64, 200–207,
9 doi:10.1016/j.atmosenv.2012.09.059, 2013.

10 Jiang, Q., Sun, Y. L., Wang, Z., and Yin, Y.: Aerosol composition and sources during the Chinese
11 Spring Festival: fireworks, secondary aerosol, and holiday effects, *Atmos. Chem. Phys.*, 15, 6023–
12 6034, doi:10.5194/acp-15-6023-2015, 2015.

13 Jimenez, J. L., Canagaratna, M. R., Donahue, N. M., Prévôt, A. S. H., Zhang, Q., Kroll, J. H.,
14 DeCarlo, P. F., Allan, J. D., Coe, H., Ng, N. L., Aiken, A. C., Docherty, K. S., Ulbrich, I. M.,
15 Grieshop, A. P., Robinson, A. L., Duplissy, J., Smith, J. D., Wilson, K. R., Lanz, V. A., Hueglin, C.,
16 Sun, Y. L., Tian, J., Laaksonen, A., Raatikainen, T., Rautiainen, J., Vaattovaara, P., Ehn, M.,
17 Kulmala, M., Tomlinson, J. M., Collins, D. R., Cubison, M. J., E, Dunlea, J., Huffman, J. A., Onasch,
18 T. B., Alfarra, M. R., Williams, P. I., Bower, K., Kondo, Y., Schneider, J., Drewnick, F., Borrmann,
19 S., Weimer, S., Demerjian, K., Salcedo, D., Cottrell, L., Griffin, R., Takami, A., Miyoshi, T.,
20 Hatakeyama, S., Shimono, A., Sun, J. Y., Zhang, Y. M., Dzepina, K., Kimmel, J. R., Sueper, D.,
21 Jayne, J. T., Herndon, S. C., Trimborn, A. M., Williams, L. R., Wood, E. C., Middlebrook, A. M.,
22 Kolb, C. E., Baltensperger, U., and Worsnop, D. R.: Evolution of organic aerosols in the atmosphere,
23 *Science*, 326, 1525–1529, 2009.

24 Lang, J.L., Cheng, S.Y., Li, J.B., Chen, D.S., Zhou, Y., Wei, X., Han, L.H., and Wang, H.Y.: A
25 monitoring and modeling study to investigate regional transport and characteristics of PM2.5
26 pollution, *Aerosol Air Qual. Res.*, 13, 943–956, 2013.

- 1 Lanz, V. A., Alfarra, M. R., Baltensperger, U., Buchmann, B., Hueglin, C., and Prévôt, A. S. H.:
2 Source apportionment of submicron organic aerosols at an urban site by factor analytical modelling of
3 aerosol mass spectra, *Atmos. Chem. Phys.*, 7, 1503-1522, doi:10.5194/acp-7-1503-2007, 2007.
- 4 ~~Lelieveld, J., Evans, J. S., Fnais, M., Giannadaki, D., and Pozzer, A.: The contribution of outdoor air
5 pollution sources to premature mortality on a global scale, *Nature*, 525, 367-371, 2015.~~
- 6 Li, H., Zhang, Q., Zhang, Q., Chen, C., Wang, L., Wei, Z., Zhou, S., Parworth, C., Zheng, B.,
7 Canonaco, F., Prévôt, A. S. H., Chen, P., Zhang, H., Wallington, T. J., and He, K.: Wintertime aerosol
8 chemistry and haze evolution in an extremely polluted city of North China Plain: significant
9 contribution from coal and biomass combustions, *Atmos. Chem. Phys.*, 17, 4751-4768,
10 doi:10.5194/acp-2016-1058, 2017.
- 11 Li, P., Yan, R., Yu, S., Wang, S., Liu, W., and Bao, H.: Reinstatement regional transport of PM_{2.5} as a
12 major cause of severe haze in Beijing, *P. Natl. Acad. Sci.*, 112, E2739-E2740,
13 doi:10.1073/pnas.1502596112, 2015a.
- 14 Li, Y. J., Lee, B. Y. L., Yu, J. Z., Ng, N. L., and Chan, C. K.: Evaluating the degree of oxygenation of
15 organic aerosol during foggy and hazy days in Hong Kong using high-resolution time-of-flight
16 aerosol mass spectrometry (HR-ToF-AMS), *Atmos. Chem. Phys.*, 13, 8739-8753, doi:10.5194/acp-
17 13-8739-2013, 2013
- 18 Li, Y. J., Lee, B. P., Su, L., Fung, J. C. H., and Chan, C. K.: Seasonal characteristics of fine
19 particulate matter (PM) based on high-resolution time-of-flight aerosol mass spectrometric (HR-ToF-
20 AMS) measurements at the HKUST Supersite in Hong Kong, *Atmos. Chem. Phys.*, 15, 37-53,
21 doi:10.5194/acp-15-37-2015, 2015b.
- 22 Middlebrook, A. M., Bahreini, R., Jimenez, J. L., and Canagaratna, M. R.: Evaluation of
23 Composition-Dependent Collection Efficiencies for the Aerodyne Aerosol Mass Spectrometer using
24 Field Data, *Aerosol Sci. Tech.*, 46, 258-271, 2012.
- 25 Minguillón, M. C., Ripoll, A., Pérez, N., Prévôt, A. S. H., Canonaco, F., Querol, X., and Alastuey, A.:
26 Chemical characterization of submicron regional background aerosols in the western Mediterranean

1 using an Aerosol Chemical Speciation Monitor, *Atmos. Chem. Phys.*, 15, 6379-6391,
2 doi:10.5194/acp-15-6379-2015, 2015.

3 Mohr, C., Huffman, J. A., Cubison, M. J., Aiken, A. C., Docherty, K. S., Kimmel, J. R., Ulbrich, I.
4 M., Hannigan, M., and Jimenez, J. L.: Characterization of primary organic aerosol emissions from
5 meat cooking, trash burning, and motor vehicles with High-Resolution Aerosol Mass Spectrometry
6 and comparison with ambient and chamber observations, *Environ. Sci. Technol.*, 43, 2443–2449,
7 doi:10.1021/es8011518, 2009.

8 Mohr, C., DeCarlo, P. F., Heringa, M. F., Chirico, R., Slowik, J. G., Richter, R., Reche, C., Alastuey,
9 A., Querol, X., Seco, R., Peñuelas, J., Jimenez, J. L., Crippa, M., Zimmermann, R., Baltensperger,
10 U., and Prévôt, A. S. H.: Identification and quantification of organic aerosol from cooking and other
11 sources in Barcelona using aerosol mass spectrometer data, *Atmos. Chem. Phys.*, 12, 1649–1665,
12 doi:10.5194/acp-12-1649-2012, 2012.

13 Ng, N. L., Canagaratna, M. R., Zhang, Q., Jimenez, J. L., Tian, J., Ulbrich, I. M., Kroll, J. H.,
14 Docherty, K. S., Chhabra, P. S., Bahreini, R., Murphy, S. M., Seinfeld, J. H., Hildebrandt, L.,
15 Donahue, N. M., DeCarlo, P. F., Lanz, V. A., Prévôt, A. S. H., Dinar, E., Rudich, Y., and Worsnop,
16 D. R.: Organic aerosol components observed in Northern Hemispheric datasets from Aerosol Mass
17 Spectrometry, *Atmos. Chem. Phys.*, 10, 4625-4641, doi:10.5194/acp-10-4625-2010, 2010.

18 Ng, N. L., Herndon, S. C., Trimborn, A., Canagaratna, M. R., Croteau, P. L., Onasch, T. B., Sueper,
19 D., Worsnop, D. R., Zhang, Q., Sun, Y. L., and Jayne, J. T.: An Aerosol Chemical Speciation Monitor
20 (ACSM) for Routine Monitoring of the Composition and Mass Concentrations of Ambient Aerosol,
21 *Aerosol Sci. Tech.*, 45, 770–784, 2011a.

22 Ng, N. L., Canagaratna, M. R., Jimenez, J. L., Zhang, Q., Ulbrich, I. M., and Worsnop, D. R.: Real-
23 time methods for estimating organic component mass concentrations from aerosol mass spectrometer
24 data, *Environ. Sci. Technol.*, 45, 910–916, 2011b.

1 Paatero, P., and Tapper, U., Positive Matrix Factorization: A Non-Negative Factor Model with
2 Optimal Utilization of Error Estimates of Data Values, *Environmetrics*, 5, 111–126, doi:
3 10.1002/env.3170050203, 1994.

4 Petit, J.-E., Favez, O., Sciare, J., Crenn, V., Sarda-Estève, R., Bonnaire, N., Močnik, G., Dupont, J.-
5 C., Haeffelin, M., and Leoz-Garziandia, E.: Two years of near real-time chemical composition of
6 submicron aerosols in the region of Paris using an Aerosol Chemical Speciation Monitor (ACSM) and
7 a multi-wavelength Aethalometer, *Atmos. Chem. Phys.*, 15, 2985-3005, doi:10.5194/acp-15-2985-
8 2015, 2015.

9 Ripoll, A., Minguillón, M. C., Pey, J., Jimenez, J. L., Day, D. A., Sosedova, Y., Canonaco, F., Prévôt,
10 A. S. H., Querol, X., and Alastuey, A.: Long-term real-time chemical characterization of submicron
11 aerosols at Montsec (southern Pyrenees, 1570 m a.s.l.), *Atmos. Chem. Phys.*, 15, 2935-2951,
12 doi:10.5194/acp-15-2935-2015, 2015.

13 Reyes-Villegas, E., Green, D. C., Priestman, M., Canonaco, F., Coe, H., Prévôt, A. S. H., and Allan, J.
14 D.: Organic aerosol source apportionment in London 2013 with ME-2: exploring the solution space
15 with annual and seasonal analysis, *Atmos. Chem. Phys.*, 16, 15545-15559, doi:10.5194/acp-16-
16 15545-2016, 2016.

17 Schlag, P., Kiendler-Scharr, A., Blom, M. J., Canonaco, F., Henzing, J. S., Moerman, M., Prévôt, A.
18 S. H., and Holzinger, R.: Aerosol source apportionment from 1-year measurements at the CESAR
19 tower in Cabauw, the Netherlands, *Atmos. Chem. Phys.*, 16, 8831-8847, [https://doi.org/10.5194/acp-](https://doi.org/10.5194/acp-16-8831-2016)
20 16-8831-2016, 2016.

21 Schneider, J., Weimer, S., Drewnick, F., Borrmann, S., Helas, G. Gwaze, P., Schmid, O., Andreae, M.
22 O., and Kirchner, U.: Mass spectrometric analysis and aerodynamic properties of various types of
23 combustion-related aerosol particles, *Int. J. Mass Spectrom.*, 258, 37–49,
24 doi:10.1016/j.ijms.2006.07.008, 2006.

1 Sun, Y. L., Wang, Z. F., Fu, P. Q., Yang, T., Jiang, Q., Dong, H. B., Li, J., and Jia, J. J.: Aerosol
2 composition, sources and processes during wintertime in Beijing, China, *Atmos. Chem. Phys.*, 13,
3 4577–4592, doi:10.5194/acp-13-4577-2013, 2013.

4 Sun, Y. L., Jiang, Q., Wang, Z., Fu, P., Li, J., Yang, T., and Yin, Y.: Investigation of the sources and
5 evolution processes of severe haze pollution in Beijing in January 2013, *J. Geophys. Res.*, 119, 4380–
6 4398, doi:10.1002/2014JD021641, 2014.

7 Sun, Y. L., Wang, Z. F., Du, W., Zhang, Q., Wang, Q. Q., Fu, P. Q., Pan, X. L., Li, J., Jayne, J., and
8 Worsnop, D. R.: Long-term real-time measurements of aerosol particle composition in Beijing, China:
9 seasonal variations, meteorological effects, and source analysis, *Atmos. Chem. Phys.*, 15, 10149–
10 10165, doi:10.5194/acp-15-10149-2015, 2015.

11 Sun, Y., Du, W., Fu, P., Wang, Q., Li, J., Ge, X., Zhang, Q., Zhu, C., Ren, L., Xu, W., Zhao, J., Han,
12 T., Worsnop, D. R., and Wang, Z.: Primary and secondary aerosols in Beijing in winter: sources,
13 variations and processes, *Atmos. Chem. Phys.*, 16, 8309–8329, doi:10.5194/acp-16-8309-2016, 2016.

14 Tie, X., Huang, R. J., Cao, J. J., Zhang, Q., Cheng, Y. F., Su, H., Chang, D., Pöschl, U., Hoffmann,
15 T., Dusek, U., Li, G. H., Worsnop, D. R., O’Dowd, C. D.: Severe pollution in China amplified by
16 atmospheric moisture, *Sci. Rep.*, 7: 15760, DOI:10.1038/s41598-017-15909-1, 2017

17 Ulbrich, I. M., Canagaratna, M. R., Zhang, Q., Worsnop, D. R., and Jimenez, J. L.: Interpretation of
18 organic components from Positive Matrix Factorization of aerosol mass spectrometric data, *Atmos.*
19 *Chem. Phys.*, 9, 2891–2918, doi:10.5194/acp-9-2891-2009, 2009.

20 Wang, G., Zhang, R., Gomez, M.E., Yang, L., Levy Zamora, M., Hu, M., Lin, Y., Peng, J., Guo, S.,
21 Meng, J., Li, J., Cheng, C., Hu, T., Ren, Y., Wang, Y., Gao, J., Cao, J., An, Z., Zhou, W., Li, G.,
22 Wang, J., Tian, P., Marrero-Ortiz, W., Secrest, J., Du, Z., Zheng, J., Shang, D., Zeng, L., Shao, M.,
23 Wang, W., Huang, Y., Wang, Y., Zhu, Y., Li, Y., Hu, J., Pan, B., Cai, L., Cheng, Y., Ji, Y., Zhang, F.,
24 Rosenfeld, D., Liss, P.S., Duce, R.A., Kolb, C.E., and Molina, M.J., Persistent sulfate formation from
25 London fog to Chinese haze, *Proc. Natl. Acad. Sci.*, 113, 13630–13635, 2016.

1 Wang, Q, Sun Y, Jiang Q, et al. Chemical composition of aerosol particles and light extinction
2 apportionment before and during the heating season in Beijing, China, *J. Geophys. Res. Atmos.*, 120,
3 12708-12722, 2015.

4 Wang, Y. C., Huang, R. J., Ni, H. Y., Chen, Y., Wang, Q. Y., Li, G. H., Tie, X. X., Shen, Z. X.,
5 Huang, Y., Liu, S. X., Dong, W. M., Xue, P., Frohlich, R., Canonaco, F., Elser, M., Daellenbach, K.
6 R., Bozzetti, C., El Haddad, I., Prevot, A. S. H.: Chemical composition, sources and secondary
7 processes of aerosols in Baoji city of northwest China, *Atmos. Environ.*, 158, 128-137, 2017.

8 Xu, X., Barsha, N.A.F. and Li, J.: Analyzing Regional Influence of Particulate Matter on the City of
9 Beijing, China, *Aerosol Air Qual. Res.*, 8, 78-93, 2008.

10 Xu, J., Zhang, Q., Chen, M., Ge, X., Ren, J., and Qin, D.: Chemical composition, sources, and
11 processes of urban aerosols during summertime in northwest China: insights from high-resolution
12 aerosol mass spectrometry, *Atmos. Chem. Phys.*, 14, 12593-12611, doi:10.5194/acp-14-12593-2014,
13 2014.

14 Xu, J., Shi, J., Zhang, Q., Ge, X., Canonaco, F., Prévôt, A. S. H., Vonwiller, M., Szidat, S., Ge, J.,
15 Ma, J., An, Y., Kang, S., and Qin, D.: Wintertime organic and inorganic aerosols in Lanzhou, China:
16 sources, processes, and comparison with the results during summer, *Atmos. Chem. Phys.*, 16, 14937-
17 14957, doi:10.5194/acp-16-14937-2016, 2016.

18 Xu, W. Q., Sun, Y. L., Chen, C., Du, W., Han, T. T., Wang, Q. Q., Fu, P. Q., Wang, Z. F., Zhao, X. J.,
19 Zhou, L. B., Ji, D. S., Wang, P. C., and Worsnop, D. R.: Aerosol composition, oxidation properties,
20 and sources in Beijing: results from the 2014 Asia-Pacific Economic Cooperation summit study,
21 *Atmos. Chem. Phys.*, 15, 13681-13698, doi:10.5194/acp-15-13681-2015, 2015.

22 Zhang, J. P., Zhu, T., Zhang, Q. H., Li, C. C., Shu, H. L., Ying, Y., Dai, Z. P., Wang, X., Liu, X. Y.,
23 Liang, A. M., Shen, H. X., and Yi, B. Q.: The impact of circulation patterns on regional transport
24 pathways and air quality over Beijing and its surroundings, *Atmos. Chem. Phys.*, 12, 5031-5053,
25 doi:10.5194/acp-12-5031-2012, 2012.

1 Zhang, R. Y., Wang, G. H., Guo, S., Zamora, M. L., Ying, Q., Lin, Y., Wang, W., Hu, M., and Wang,
2 Y.: Formation of urban fine particulate matter, *Chem. Rev.*, 115, 3803–3855,
3 doi:10.1021/acs.chemrev.5b00067, 2015a.

4 Zhang, Y. J., Tang, L. L., Wang, Z., Yu, H. X., Sun, Y. L., Liu, D., Qin, W., Canonaco, F., Prévôt, A.
5 S. H., Zhang, H. L., and Zhou, H. C.: Insights into characteristics, sources, and evolution of
6 submicron aerosols during harvest seasons in the Yangtze River delta region, China, *Atmos. Chem.*
7 *Phys.*, 15, 1331-1349, doi:10.5194/acp-15-1331-2015, 2015b.

8 Zhang, Y. J., Tang, L. L., Yu, H. X., Wang, Z., Sun, Y. L., Qin, W., Chen, W. T., Chen, C. H., Ding,
9 A. J., Wu, J., Ge, S., Chen, C., and Zhou, H. C.: Chemical composition, sources and evolution
10 processes of aerosol at an urban site in Yangtze River Delta, China during wintertime, *Atmos.*
11 *Environ.*, 123, 339-349, 2015c.

12 Zhao, P., Dong, F., Yang, Y., He, D., Zhao, X., Zhang, W., Yao, Q., and Liu, H.: Characteristics of
13 carbonaceous aerosol in the region of Beijing, Tianjin, and Hebei, China, *Atmos. Environ.*, 71, 389–
14 398, 2013a.

15 Zhao, P. S., Dong, F., He, D., Zhao, X. J., Zhang, X. L., Zhang, W. Z., Yao, Q., and Liu, H. Y.:
16 Characteristics of concentrations and chemical compositions for PM_{2.5} in the region of Beijing,
17 Tianjin, and Hebei, China, *Atmos. Chem. Phys.*, 13, 4631–4644, doi:10.5194/acp-13-4631-2013,
18 2013b.

19 Zhou, W., Jiang, J., Duan, L., and Hao, J.: Evolution of submicron organic aerosols during a complete
20 residential coal combustion process, *Environ. Sci. Technol.*, 50, 7861–7869, 2016.

21 [Zhu, Q., Huang, X.-F., Cao, L.-M., Wei, L.-T., Zhang, B., He, L.-Y., Elser, M., Canonaco, F., Slowik,](#)
22 [J. G., Bozzetti, C., El-Haddad, I., and Prévôt, A. S. H.: Improved source apportionment of organic](#)
23 [aerosols in complex urban air pollution using the multilinear engine \(ME-2\), *Atmos. Meas. Tech.*, 11,](#)
24 [1049-1060, <https://doi.org/10.5194/amt-11-1049-2018>, 2018.](#)

25

1

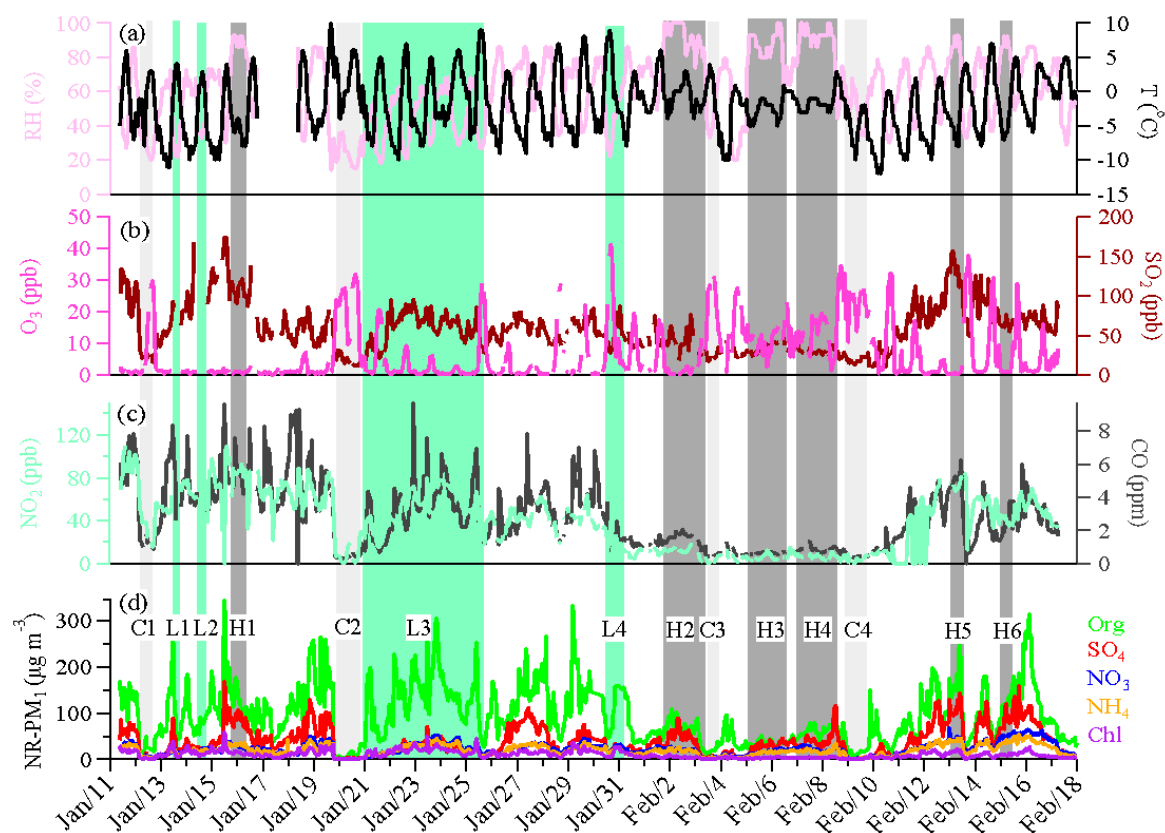
2

3 Table 1. The fine PM mass concentrations and fractional contribution of different composition in
 4 different locations.

City	Season	NR-PM ₁ ($\mu\text{g m}^{-3}$)	OA %	SO ₄ ²⁻ %	NO ₃ ⁻ %	NH ₄ ⁺ %	Cl ⁻ %	Ref.
Beijing	Winter, 2010	60	54	14	11	12	9	Hu et al., 2016a
Beijing	Winter, 2011	59	51	13	17	14	5	Sun et al., 2015
Beijing	Winter, 2012	66.8	52	14	16	13	5	Sun et al., 2013
Beijing	Winter, 2012	79	52	17	14	10	7	Wang et al., 2015
Beijing	Winter, 2013	77	50	19	16	12	3	Sun et al., 2014
Beijing	Winter, 2013	13.0	52	17	14	10	7	Jiang et al., 2015
Beijing	Winter, 2013	64	60	15	11	8	6	Sun et al., 2016
Beijing	Winter, 2014	75 ^a	56	16	10	7	11	Elser et al., 2016
Beijing	Summer, 2011	80	32	28	21	17	2	Hu et al., 2016a
Beijing	Summer, 2012	52	41	14	25	17	3	Sun et al., 2015
Lanzhou	Winter,	57.3	55	13	18	11	3	Xu et al., 2016

Lanzhou	2014 Summer, 2012	24	53	18	11	13	5	Xu et al., 2014
Ziyang	Winter, 2012	60	40	24	15	17	4	Hu et al., 2016b
Handan	Winter, 2015	178	47	16	15	13	9	Li et al., 2017
Shenzhen	Autumn, 2009	38.3	46	29	12	11	2	He et al., 2011
Shanghai	Summer, 2010	27	31	36	17	14	2	Huang et al., 2012
Nanjing	Summer, 2013	36.8	42	14	24	19	1	Zhang et al., 2015b
Hong Kong	Winter, 2012	14.5	33	40	10	16	1	Li et al., 2015b
Hong Kong	Summer, 2011	8.7	26	56	3	15	0.1	Li et al., 2015b
Paris	Winter, 2010	16.7	35	16	33	15	1	Crippa et al., 2013
Fresno, California	Winter, 2010	11.8	67	3	20	8	2	Ge et al., 2012
Shijiazhuang	Winter, 2014	178	50	21	12	11	6	This study

1 ^aNR-PM_{2.5}

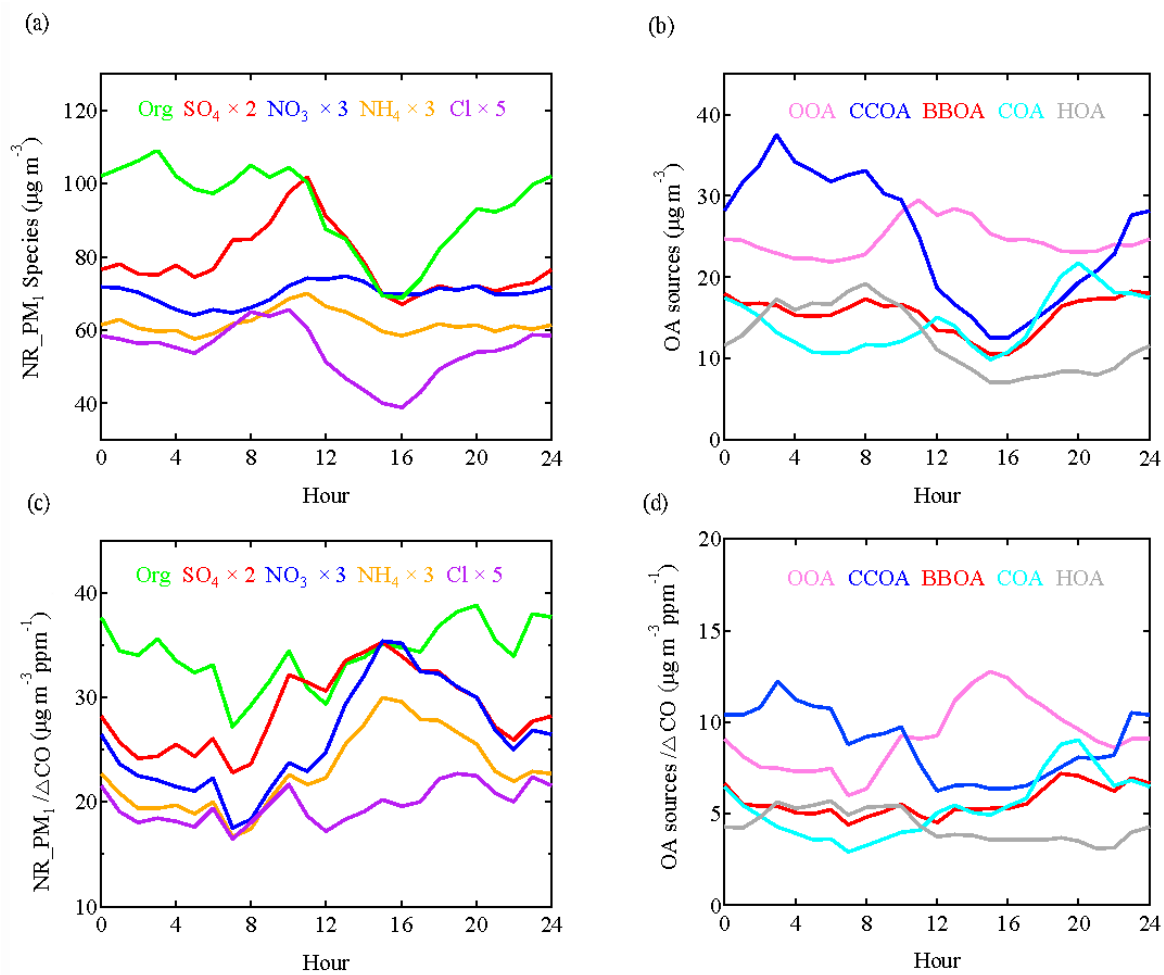


1

2 **Fig. 1** Time series of relative humidity and temperature(a), O₃ and SO₂ (b), NO₂ and CO (c),
 3 and the NR-PM₁ species (d) during the observation period. 6 high-RH (>80%) polluted episodes
 4 (H1-H6), 4 low-RH (<60%) polluted episodes (L1-L4), and 4 clean episodes (C1-C4) are marked
 5 for further discussion.

6

7

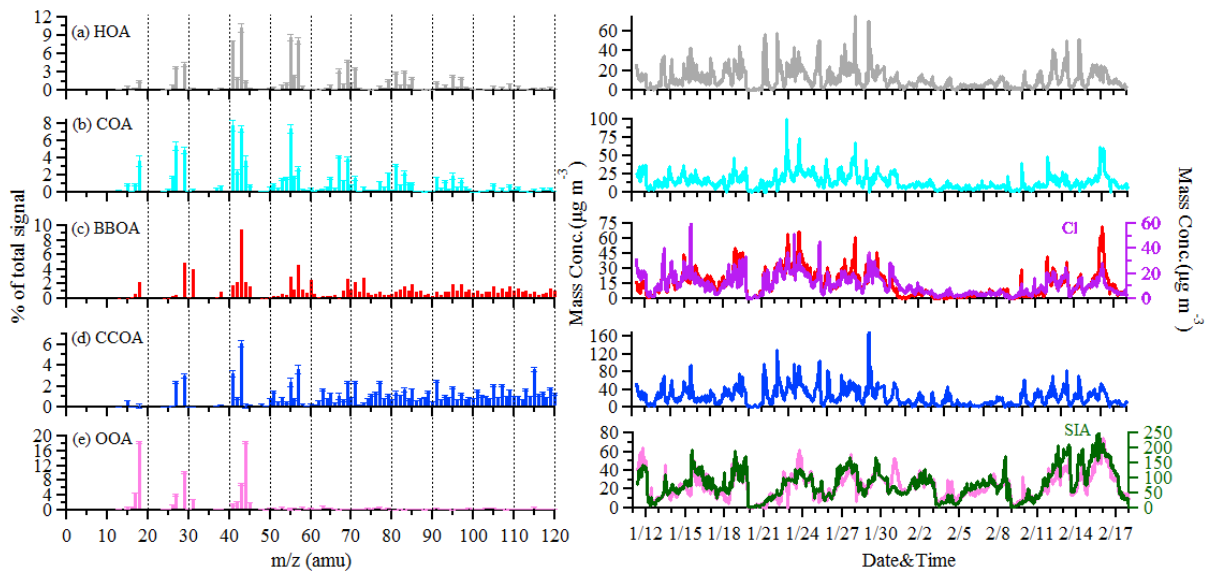


1

2 **Fig. 2. Diurnal variations of NR-PM₁ composition (a), OA sources (b), NR-PM₁ species/ΔCO (c)**
 3 **and OA sources/ΔCO (d).**

4

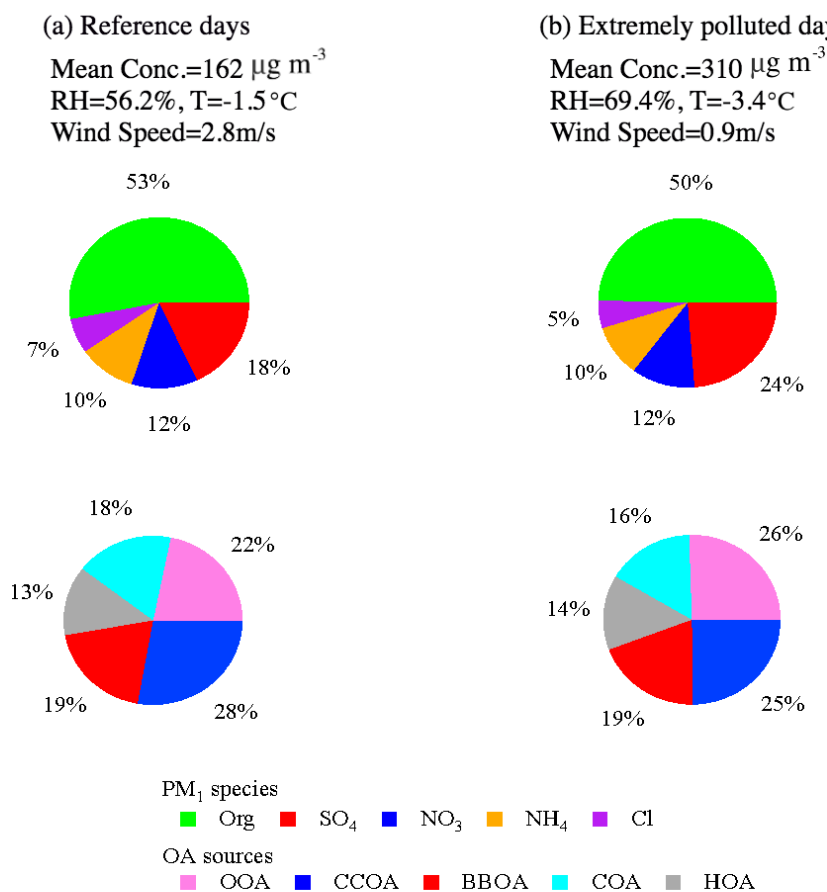
5



1

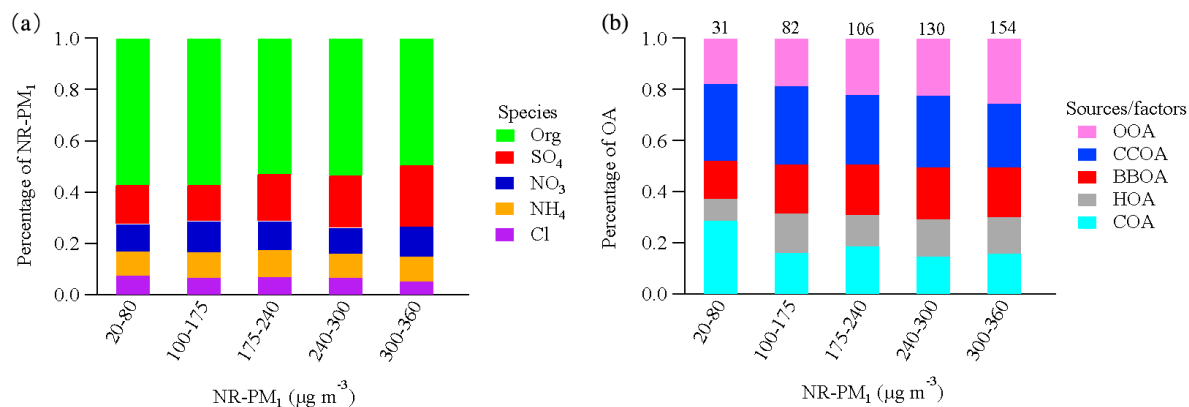
2 **Fig. 3** Mass spectrums (left) and time series (right) of five OA sources. Error bars of mass
 3 spectrums represent the standard deviation of each m/z over all accepted solutions.

4



1
 2
 3
 4
 5
 6
 7

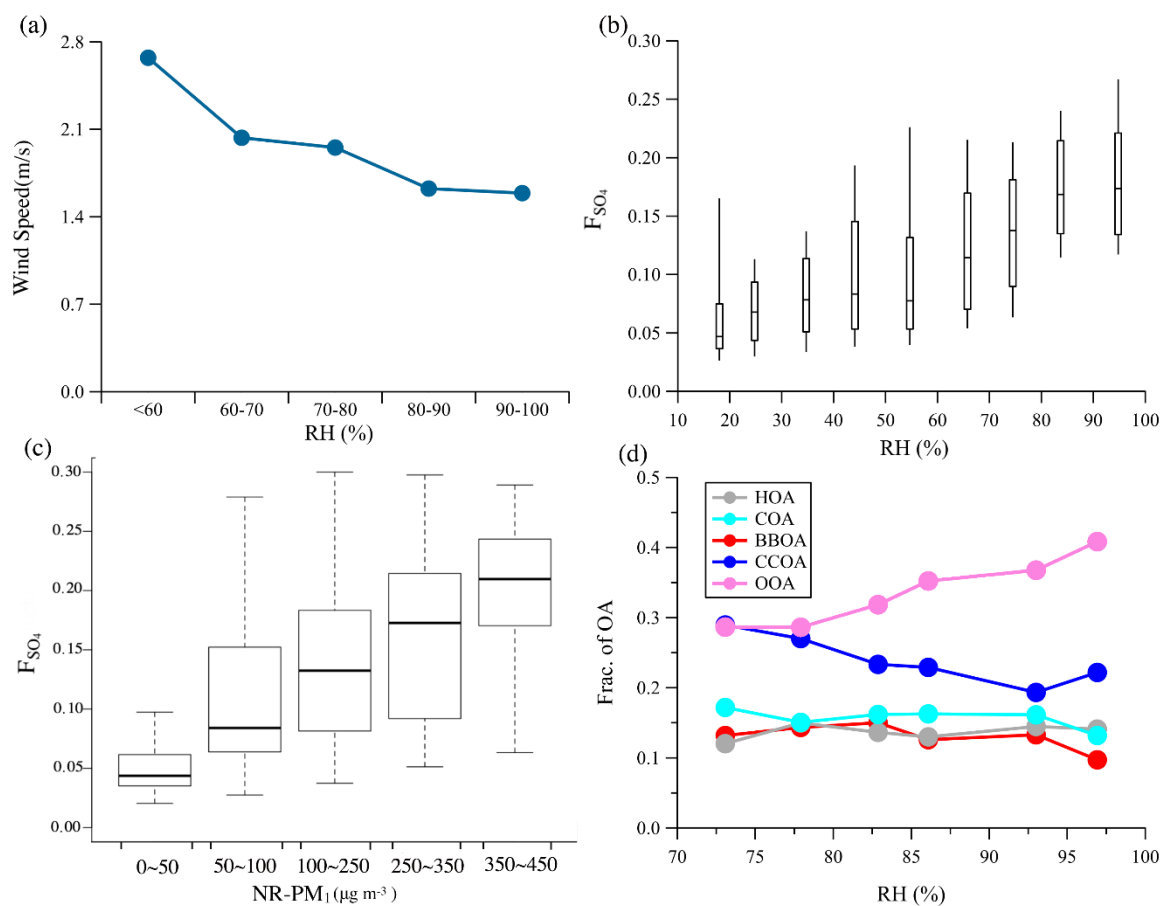
Fig. 4. Relative contributions of NR-PM₁ species and OA sources (OOA, CCOA, BBOA, COA and HOA) in reference days (a) and extremely polluted days (b). Extremely polluted days are defined as the daily average mass concentration of NR-PM₁ higher than the 75th percentile (237.3 $\mu\text{g m}^{-3}$) and the rest refers to the reference days. Data in the Spring Festival is excluded to eliminate the influence from a change of emission patterns in the holiday.



1

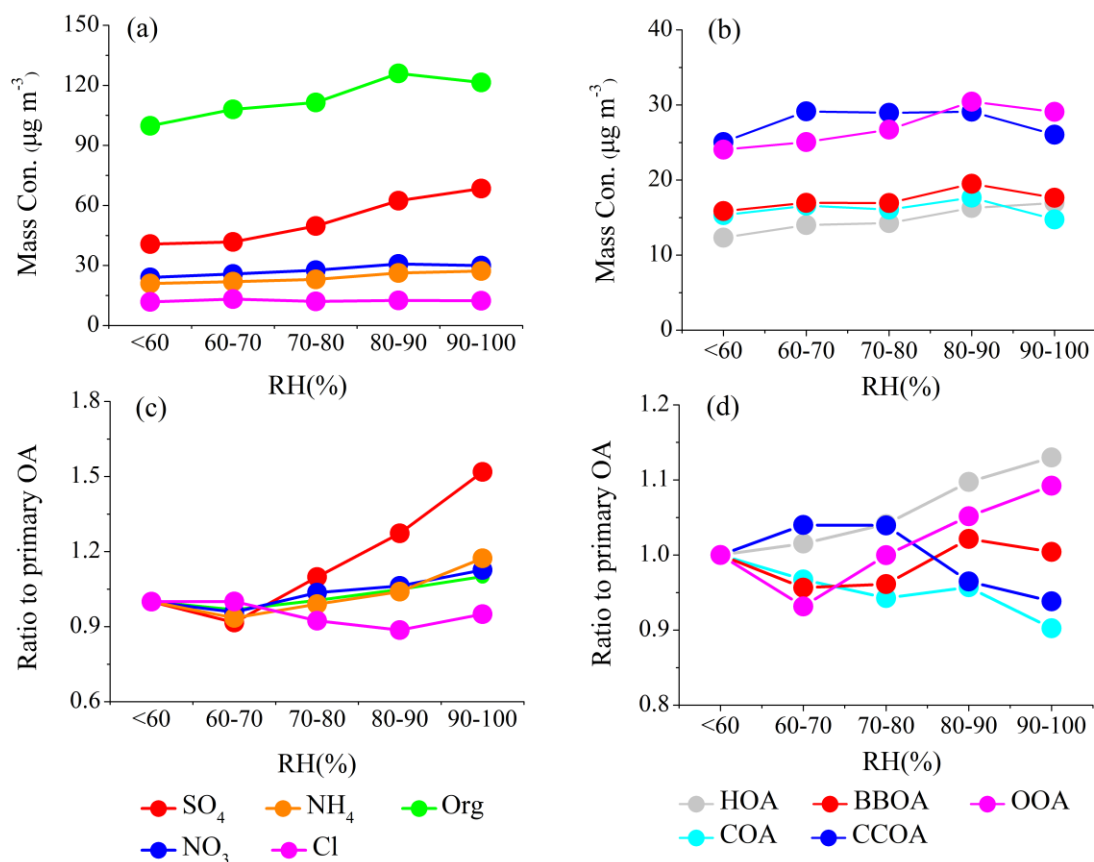
2 **Fig. 5. Relative contributions of NR-PM₁ species (a) and OA sources (b) as a function of daily**
 3 **average NR-PM₁ mass concentrations. The numbers above the bars refer to the OA mass**
 4 **concentration (µg m⁻³). Data in the Spring Festival is excluded to eliminate the influence from**
 5 **the change of emission patterns in the holiday.**

6



1

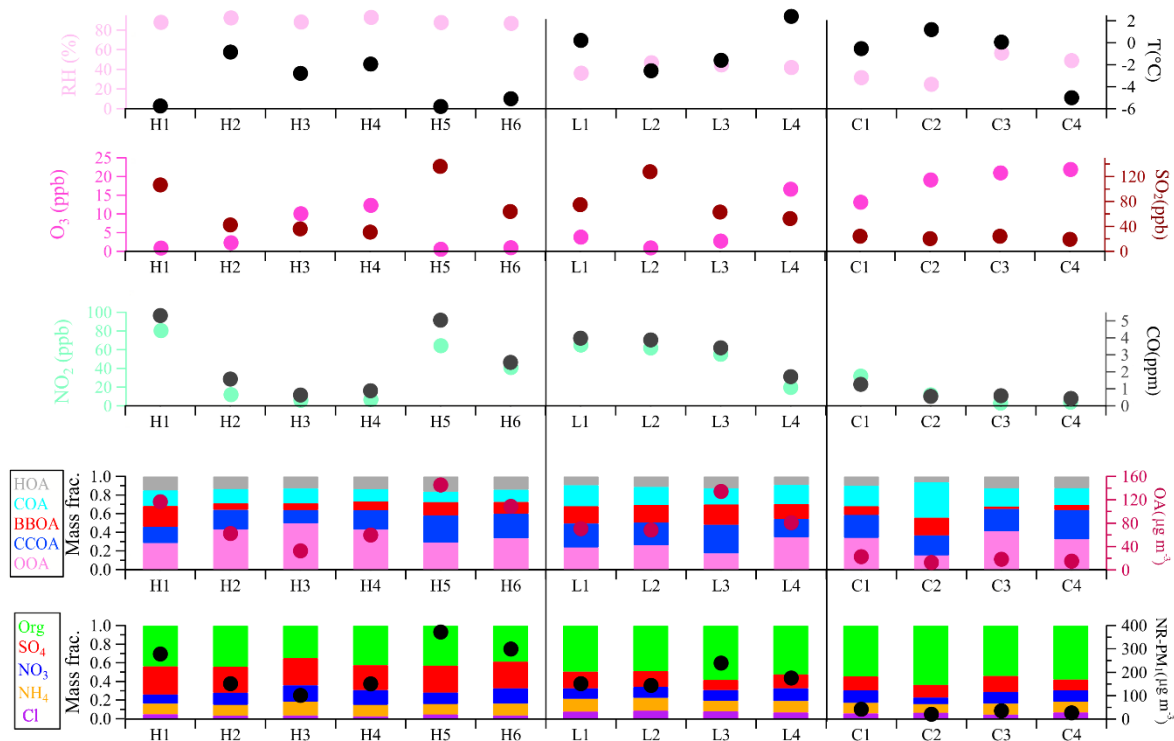
2 **Fig. 6.** Variations of wind speed as a function of RH (a), F_{SO_4} as a function of RH (b) and of the
 3 NR- PM_{10} mass concentrations (c), and the mass fraction of organic as a function of RH (d).



1

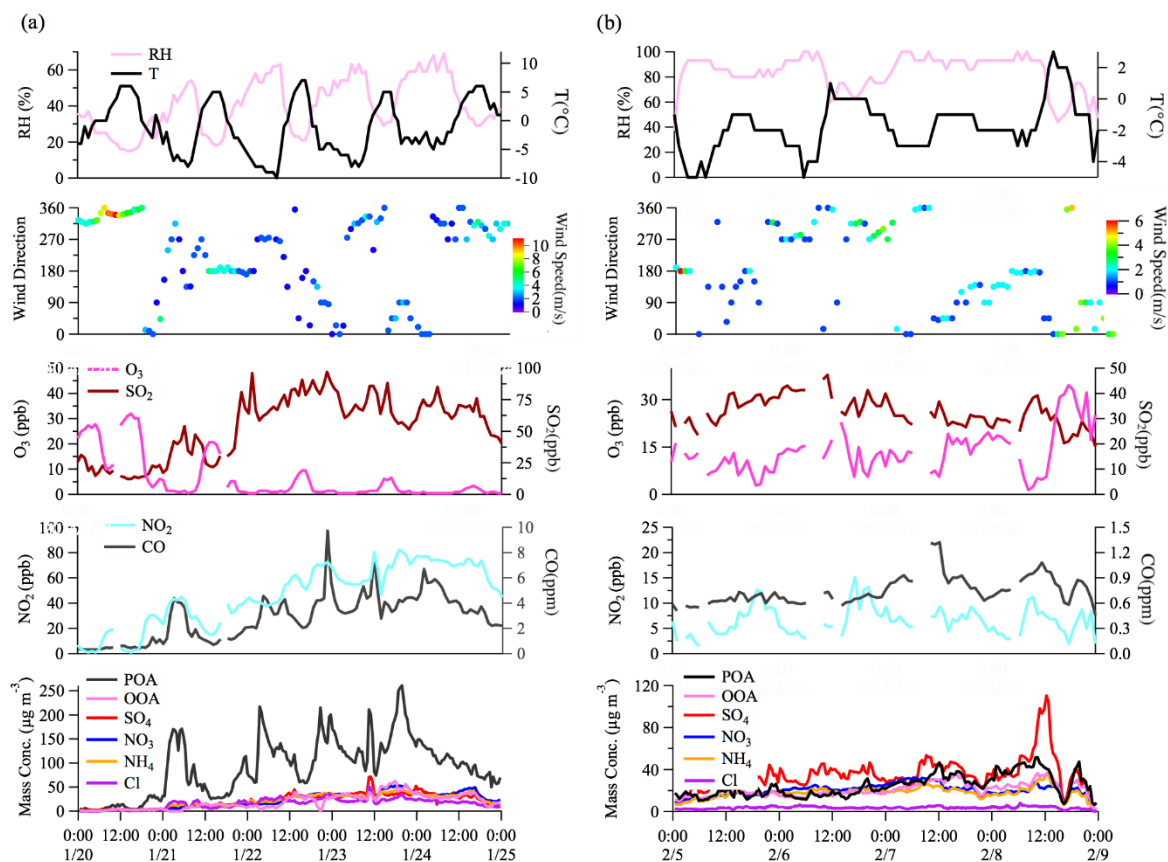
2 **Fig. 7. The average mass concentration of NR-PM₁ species (a) and OA sources (b) as a function**
 3 **of RH. The average mass concentration of NR-PM₁ species (c) and OA sources (d) normalized**
 4 **to the sum of primary sources (HOA, COA, BBOA, and CCOA) as a function of RH. All ratios**
 5 **are further normalized to the values at the first RH bin (<60%) for the better illustration.**

6



1

2 **Fig. 8. Summary of relative humidity and temperature, gaseous species, organic sources and**
 3 **NR-PM₁ chemical composition for high-RH (H1-H6) polluted, low-RH (L1-L4), and clean (C1-**
 4 **C4) episodes.**



1
 2 **Fig. 9. Time series of meteorological factors (relative humidity, temperature, wind speed and**
 3 **wind direction), gaseous species, OA factors and NR-PM₁ chemical composition for the first**
 4 **period (average RH <50%) (a) and the second period (average RH >80%) (b).**